Physics – Uspekhi **63** (2) 123 – 144 (2020)

REVIEWS OF TOPICAL PROBLEMS PACS numbers: 03.75.Kk, 05.45.Xt, **05.65.+b**, 42.65.Sf, 47.20.Ky, **71.36.+c**

Nonequilibrium transitions, chaos, and chimera states in exciton–polariton systems

S S Gavrilov

DOI: https://doi.org/10.3367/UFNe.2019.04.038549

Contents

1. Introduction **123**
2. Polaritons in a microcavity **125**
3. Multistability of polariton condensate **127**
4. Bogolyubov quasiparticles **128**
5. Regime with blowup **130**
5.1 Theoretical analysis; 5.2 Numerical example; 5.3 Experiments
6. Break-up of a condensate with nonzero momentum **132**
6.1 Parametric scattering; 6.2 Rayleigh scattering and superfluidity
7. Spin symmetry breaking **134**
7.1 Theoretical analysis; 7.2 Experiments
8. Chaos and a new order **137**
8.1 Turbulence in optics; 8.2 Loop scattering mechanism; 8.3 Self-pulsations and deteministic chaos; 8.4 Filaments; 8.5 Dipolar spin network; 8.6 Chimera states
9. Conclusions **142**
References **143**

Abstract. The review is devoted to exciton polaritons, short-lived Bose particles which are optically excited in semiconductors and form macroscopically coherent states under conditions of coherent and resonant external driving. The interaction of polaritons results in multistability, spontaneous breaking of spin and spatial symmetries, self-pulsations, and pattern formation. As a result of symmetry breaking, paradoxical 'chimera states' can arise in which ordered and chaotic subsystems coexist and in some way complement each other.

Keywords: polariton, Bose–Einstein condensate, spinor condensate, multistability, spontaneous symmetry breaking, self-pulsations, dynamical chaos, chimera states, self-organization

1. Introduction

An exciton is a bound pair of mutually attracting electron and hole in a semiconductor, similar to a positronium atom. Excitons are excited by light and recombine emitting light. Excitons and photons in certain cases transform into each other with such a frequency that they cannot be distinguished separately; should this be the case, the concept of new quasiparticles — exciton polaritons — is used [1]. Of particular interest are two-dimensional polaritons trapped in a thin layer of a planar microcavity [2-4]. Being initially in a disordered state, with decreasing temperature they form a Bose–Einstein condensate that emits coherent light [5]. However, a reverse process is also possible when light with the same wavelength, being absorbed, excites a coherent polariton state — a nonequilibrium analogue of the Bose condensate.

The phase transitions associated with the emergence of coherence under equilibrium conditions are rather well studied in such systems as superfluid liquid helium, superconducting metals, and atoms cooled in magnetic traps [6]. A multitude of indistinguishable particles acquires in all these systems the properties of a classical field characterized by a common amplitude and a spontaneously chosen phase. The critical temperature of Bose–Einstein condensation is inversely proportional to the mass of particles and, for ordinary atoms, is in the region of 10^{-8} K. Quasi-two-dimensional polaritons have a very small mass, even in comparison with free electrons, and, depending on the sample material, condense at temperatures ranging from several kelvins [7, 8] to room temperature [9–11]. This circumstance, combined with an exceptional simplicity of the experiment in which the amplitude and phase of the condensate are seen almost immediately in the emitted coherent light, were the features that attracted much attention to polaritons [5, 12, 13]. The topics that are currently studied in this field include transport of excitations in tunnel-coupled traps and Josephson oscillations [14, 15], quantized vortices [16–19], and 'simulators' of

S S Gavrilov
Institute of Solid State Physics, Russian Academy of Sciences,
ul. Akademika Osip'yana 2, 142432 Chernogolovka, Moscow region,
Russian Federation;
National Research University Higher School of Economics,
ul. Myasnitskaya 20, 101000 Moscow, Russian Federation
E-mail: gavr_ss@issp.ac.ru

Received 6 September 2018, revised 3 April 2019
Uspekhi Fizicheskikh Nauk **190** (2) 137 – 159 (2020)
Translated by M Zh Shmatikov; edited by the author

optimization problems based on distributed systems that tend to equilibrium [20].

The second area of research, which is primarily reviewed here, is the nonequilibrium condensation of polaritons under coherent optical driving. The possibility of nonequilibrium condensation was explored as early as 1972 by L V Keldysh [21, 22], V F Elesin, and Yu V Kopaev [23]. It was as late as 2006 that it was experimentally established that two-dimensional polaritons excited by a resonant plane wave indeed form a common 'single-particle' quantum state [24]. There is neither critical termperature nor even thermal equilibrium, and the light wave performs as the direct source of the coherent state.

Regardless of the condensation origin and conditions, the coherent state can be described within the mean-field approximation using a macroscopic wave function ψ that satisfies Ginzburg–Landau-type equations $\mathrm{i}\hbar\partial_t\psi = \delta H/\delta\psi^*$. Hamiltonian H usually contains a term of the form $H_{\mathrm{int}}(\mathbf{r}) = (V/2)|\psi(\mathbf{r})|^4$, $V > 0$, which corresponds to the pairwise repulsion of particles in a dilute gas [4, 6]. If the system of polaritons is excited by a resonant external field, it combines in a certain sense the condensate and a dissipative oscillator excited by an external force; however, its behavior cannot be reduced to a simple combination of the features of the known models. Formally similar equations are also used to describe some nonlinear optical systems [25], but, in contrast to them, polaritons have a positive mass, move freely in two dimensions, and experience elastic scattering.

Most importantly, the nonequilibrium condensate of polaritons can be controlled by varying the external field. Being relatively weak, it completely determines the condensate state, but as the amplitude grows, nonlinearity leads to the excitation of above-condensate modes and a variety of collective effects. In particular, the response of polaritons to a light wave can be multiple-valued. At special critical points, the amplitude ψ — and with it the radiation from the cavity backside — experiences jumps between the stability branches [26–34], owing to which the system behaves like a multistable cell with a characteristic switching time of the order of several picoseconds in GaAs-based samples [35]. The condensate break-up also occurs in a threshold manner, resulting in the onset of new coherent modes [36–44]. The strong exciton–photon coupling allows combining the compactness characteristic of electronic devices and the 'photonic' speed; therefore, the nonequilibrium transitions discussed here are often explored in the context of developing new optical switches and logic elements, an example of which is the prototype of a polariton transistor [45].

In studying condensates and quantum liquids, a question usually arises of the energy levels of above-condensate modes $\tilde{E}$ as functions of the wave number k. The dispersion law $\tilde{E}(k)$ is renormalized with a change in amplitude ψ. N N Bogolyubov was the first to show that a 'sound' excitation spectrum $\tilde{E} \propto k$ should arise near the equilibrium condensate, which leads to superfluidity in accordance with the Landau criterion [46]. The external field brings about a new parameter to the theory, as a result of which the excitation spectra are much more diverse; for example, they can have a gap near the condensate mode. The superfluidity effect, which was observed in a nonequilibrium polariton system [47–49], occurs in it in a threshold manner as the pump amplitude increases.

Another consequence of the modification of Bogolyubov spectra is the unusual features of the polariton–polariton scattering. If the frequency of the external field is higher than that of the polariton resonance, the break-up of the condensate $(\mathbf{k}, \mathbf{k}) \to (\mathbf{k}', 2\mathbf{k} - \mathbf{k}')$ is accompanied not by a decrease, but by an increase in its own amplitude $|\psi(\mathbf{k})|$, despite the scattering is elastic. The energy of the system grows until the blue shift of the resonance compensates this difference in frequencies, and many modes with various momenta $\hbar\mathbf{k}'$ are concurrently populated [50, 51]. The transitional state, in which the amplitude of each of the scattered modes is still small but whose total population and the feedback effect on the condensate are significant, exhibits in experiments strong quantum noise and a nontrivial spatial structure [52].

In a number of cases, all the states in which the condensate-mode momentum takes any certain value are unstable. A spontaneous violation of spatial symmetry then occurs, and the distribution $\psi(\mathbf{r})$ evolves chaotically all the time [53] or, on the contrary, forms an inhomogeneous regular structure featuring a long-range order [54]. It is noteworthy that dissipative structures and chaos arise in a simple homogeneous system of short-lived and repulsive particles, although such systems usually adiabatically follow the external field, despite even nonlinearity.

For clarity, let us consider a planar system of polaritons that is excited by a light wave incident along the normal direction (z axis). The light wave creates a zero-momentum condensate in the xy plane. Polaritons whose projection J_z of the total angular momentum equals $+1$ (-1) correspond to photons with a right-handed (left-handed) circular polarization. These two spin components do not usually interact pairwise, but they can be linearly coupled due to the splitting of the initial eigenstates [55]. The wave equations for ψ_+ and ψ_- then take the form

$$\mathrm{i}\hbar\frac{\partial\psi_\pm}{\partial t} = \left(\hat{E} - \mathrm{i}\gamma + V\psi_\pm^*\psi_\pm\right)\psi_\pm + \frac{g}{2}\,\psi_\mp + f_\pm \exp\left(-\frac{\mathrm{i}E_\mathrm{p}t}{\hbar}\right), \tag{1}$$

where $\hat{E} = \hat{E}(-\mathrm{i}\hbar\nabla)$ is the polariton energy with consideration for the dispersion law, γ is the decay rate, $g/2$ is the coupling constant of the spin components, and $E_\mathrm{p}/\hbar$ is the pump frequency chosen near the eigenfrequency of the polariton mode $k = 0$.

It is apparent that if the external field is spin-symmetric ($f_+ = f_-$), then the equations for ψ_+ and ψ_- are completely identical. It turns out, however, that if $g \gtrsim \gamma$, the symmetry is inevitably broken in a finite region of the parameters f and E_p. In this case, as the amplitude f increases, the light emitted by polaritons acquires at some moment of time an almost complete right- or left-handed circular polarization [55–57]. If, however, $g > 4\gamma$, it may turn out that there are no stable single-mode states of the type $\psi_\pm(t) = \bar{\psi}_\pm \exp(-\mathrm{i}E_\mathrm{p}t/\hbar)$ at all, and then spatiotemporal chaos sets in. Two channels of polariton interaction, pair scattering and linear coupling of spin components, form in this case a hybrid loop process [58].

Optical chaos is applied in secure communications [59, 60]. The sources of chaotic radiation known today are relatively complicated and imply the presence of an active medium where light is generated or amplified, of external feedback, etc. A polariton system is much simpler: it enables generation of a chaotic signal merely by passing a light wave through a very thin (0.1 mm) heterostructure. The characteristic oscillation frequency of the intensity and polarization of light can, as a result, reach 10^{11} Hz, a value that is significantly greater than in laser emitters, provided that a deterministic and continuous, rather than random, signal is meant.

Spatiotemporal chaos resembles turbulence. Solutions of Eqns (1) for 2D systems exhibit a periodic filamentary structure in which filaments with opposite polarizations alternate each other [53].

A completely new phenomenon arises in analogous one-dimensional systems. In this case, a periodic network is formed in which the areas with spins $+1$ and -1 alternate, being separated by relatively narrow gaps with a low total intensity $|\psi_+|^2 + |\psi_-|^2$. Regardless of spin, some nodes of this network oscillate in phase with each other and with the external field, while the other nodes oscillate randomly, the fraction of both subsystems being approximately being constant in time and independent of the size of the system. However, the balance between order and disorder is dynamic, so that individual nodes or their small groups sometimes unpredictably pass from one subsystem to another. By changing the parameters, a continuous transition from a periodic lattice with spontaneously arising rigid long-range order to fully developed turbulence may be traced [54].

States with very similar properties, so-called chimera states that occur spontaneously and combine order and disorder, have been found in a wide variety of dynamic systems and attract growing interest. They were predicted by Y Kuramoto in 2002 in the context of a coupled phase-oscillator model [61–65]:

$$\frac{\partial\phi(x,t)}{\partial t} = \omega - \int G(x-x')\sin\left[\phi(x,t) - \phi(x',t) + \alpha\right] \mathrm{d}x', \quad (2)$$

with a nearly homogeneous initial state and nonlocal interaction, for example, $G(d) \propto \exp(-\varkappa|d|)$. Chimera states have been found quite recently in emission from feedback lasers [66, 67] as well as mechanical [68] and chemical [69] systems; they are also discussed in the context of neurophysiology [70, 71]. Study [54], the discussion of which completes this review, contains the first theoretical evidence of chimera states in a basic system of locally interacting Bose particles.

2. Polaritons in a microcavity

An electron–hole pair produced by the absorption of a photon in a semiconductor can be bound by Coulomb attraction. Bound states — Wannier excitons — have a ground-state energy

$$E_{\mathrm{X}} = E_{\mathrm{g}} - \frac{\hbar^2}{2m_{\mathrm{X}}a^2}, \quad (3)$$

where E_{g} is the band gap, m_{X} is the reduced mass, $a = \varepsilon\hbar^2/m_{\mathrm{X}}e^2$ is the Bohr radius, and ε is the dielectric constant. Excitons are subject in the low-density limit to Bose–Einstein statistics and are indistinguishable [72]; therefore, in principle, they can experience Bose condensation [21, 22, 73].

However, *polariton* condensates in three-dimensional (bulk) semiconductors are not formed, since the photons have there the linear dispersion law $E = \hbar c k_{3\mathrm{D}}/\sqrt{\varepsilon}$ and, therefore, there is no ground state that could be populated under condensation. On the other hand, even in an external field with suitable E and $k_{3\mathrm{D}}$ that excites some of the nonground states, polaritons inevitably interact with the atomic environment: they collide with phonons, scatter on all kinds of heterogeneities of the structure, etc. It can be asserted that the work of Elesin and Kopaev [23], where Bose condensation in an external field was predicted, was way ahead of its time.

The situation crucially changes if the excitons are trapped in a two-dimensional quantum well and the well itself is placed into a Fabry–Pérot-type planar microcavity [3]. A microcavity 'tuned' to the λ wavelength is formed by two Bragg mirrors, each of which consists of alternating flat layers with slightly different thicknesses $l_{1,2}$ and refractive indices $n_{1,2}$, namely such that $n_1 l_1 = n_2 l_2 = \lambda/4$. This is the Bragg reflection condition, i.e., equality of the phase for waves reflected from identical interfaces. As the number of such pairs of layers in an individual mirror increases, its transmission exponentially decreases in a certain wavelength band near λ, the width of which is $\Delta\lambda = 2\lambda|n_1 - n_2|/(\pi n)$, where $n = \sqrt{\varepsilon} = 2n_1n_2/(n_1 + n_2)$. Two mirrors are separated by an *active layer*. If the optical thickness of the active layer is an integer multiple of $\lambda/2$, the maximum of the electric field of the standing wave that emerges between the mirrors is located in its middle. The standing wave has a very narrow ($\ll \Delta\lambda$) resonance at length λ. The wave vector component of the standing wave, which is orthogonal to the cavity, is fixed by the condition $k_z = \pm 2\pi n/\lambda$; however, the spectrum of the longitudinal component $k = \sqrt{k_x^2 + k_y^2}$ remains unrestricted. Thus, the dispersion law of 'cavity' photons has the form

$$E_{\mathrm{C}}(k) = \frac{\hbar c}{n}\sqrt{k^2 + k_z^2} \approx E_0 + \frac{\hbar^2 k^2}{2m}, \qquad k \ll k_z, \quad (4)$$

where $E_0 = 2\pi\hbar c/\lambda$ and $m = \varepsilon E_0/c^2$. If $n_{1,2}$ and $l_{1,2}$ are properly selected, E_0 may be set near the exciton energy, whereas k is determined by the light-wave incidence angle θ: $k = k_{3\mathrm{D}}\sin\theta$. The radiation emerging from the other side of the cavity carries information about the field in the active layer, since the mirrors themselves do not introduce nonlinearity.

A planar quantum well with excitons is located in the electric field antinode; it is nothing but an even thinner homogeneous layer of another material whose thickness is less than the 3D exciton Bohr radius. The eigenenergy of 2D excitons $E_{\mathrm{g}} - E_{\mathrm{X}}$ is four times higher, and therefore they are effectively confined in their layer. The strength of the exciton–photon coupling can be enhanced if several planar wells separated by barriers, rather than one, are created [3, 74].

The Hamiltonian operator of the linearly coupled exciton-photon system where zero-state oscillations and spin are disregarded has the form

$$\mathcal{H} = \sum_{\mathbf{k}}\left[E_{\mathrm{C}}(\mathbf{k})\, a_{\mathbf{k}}^{\dagger}a_{\mathbf{k}} + E_{\mathrm{X}}(\mathbf{k})\, b_{\mathbf{k}}^{\dagger}b_{\mathbf{k}} + \frac{R}{2}\left(a_{\mathbf{k}}^{\dagger}b_{\mathbf{k}} + b_{\mathbf{k}}^{\dagger}a_{\mathbf{k}}\right)\right], \quad (5)$$

where $a_{\mathbf{k}}$ and $b_{\mathbf{k}}$ are the annihilation operators of photons and excitons with wave number $\mathbf{k}$. Diagonalization of expression (5) yields eigenenergies

$$E_{\mathrm{LP,UP}}(\mathbf{k}) = \frac{1}{2}\left[E_{\mathrm{C}}(\mathbf{k}) + E_{\mathrm{X}}(\mathbf{k})\right] \mp \frac{1}{2}\sqrt{\left[E_{\mathrm{C}}(\mathbf{k}) - E_{\mathrm{X}}(\mathbf{k})\right]^2 + R^2} \quad (6)$$

of the lower (LP) and upper (UP) polariton states. Exciton–photon coupling results in a characteristic splitting of the spectra. It is seen, in particular, that if $E_{\mathrm{C}} = E_{\mathrm{X}}$, the eigenenergies are split by the quantity R, which is referred to as Rabi splitting (Fig. 1).

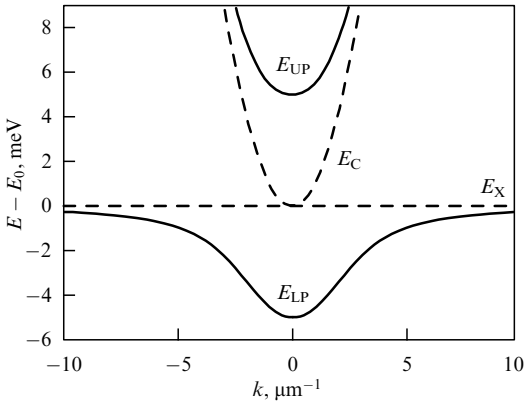

Figure 1. Dispersion law of quasi-two-dimensional exciton polaritons ($\varepsilon = 12$, $E_0 = E_X = 1.6$ eV, $R = 10$ meV).

Below, the characteristic values of the parameters are presented using the example from [57]. GaAs and AlAs are used as the main materials, and the resonance energy of photons E_0 is approximately 1.6 eV. Each mirror consists of more than 30 pairs of quarter-wave AlAs and $Al_{0.2}Ga_{0.8}As$ layers, which provides a Q-factor of about 10^4. The optical thickness of the active layer (AlAs) is $\lambda/2$. Seven 7-nm-thick quantum wells (GaAs) are separated by 4-nm-thick barriers (AlAs). The Rabi splitting is 10 meV, which is approximately two orders of magnitude greater than the spectral width of the resonances at the liquid-helium temperature.

The effective photon mass $m = \varepsilon E_0/c^2$ is extremely small ($E_0 \sim E_X \lesssim E_g$). The exciton can be considered infinitely heavy compared to the photon, and the dependence of E_X on k near $k = 0$ can be ignored. A 'bottleneck' emerges in the $E_{LP}(k)$ spectrum, a steep but not very long segment in which the probability of colliding with phonons is very low. By this reason, the polaritons excited by coherent light near the bottom of $E_{LP}(k)$ also form a coherent state [24, 75]. Another way for the coherent states to emerge is through a conventional Bose condensation from the exciton reservoir, which can be created by *nonresonant* pumping with the frequency $\omega > E_g/\hbar$ [5, 7, 8, 12]. The upper polariton branch is in both cases empty and, as a rule, it can be disregarded.

If the interaction between polaritons is not taken into account, their coherent state with wave number $\mathbf{k}$ has the form

$$\Phi_{\mathbf{k}} = \exp\left(-\frac{|\psi_{\mathbf{k}}^2|}{2} + \psi_{\mathbf{k}} p_{\mathbf{k}}^{\dagger}\right)|0\rangle\,,$$

where $p_{\mathbf{k}}$ is the bosonic annihilation operator and $\psi_{\mathbf{k}}$ is the complex-valued amplitude. By virtue of the known property $p_{\mathbf{k}}\Phi_{\mathbf{k}} = \psi_{\mathbf{k}}\Phi_{\mathbf{k}}$, the Heisenberg equation for $p_{\mathbf{k}}$ transforms after averaging over $\Phi_{\mathbf{k}}$ into the Hamilton equation $\partial_t\psi_{\mathbf{k}} = \delta H/\delta(\mathrm{i}\hbar\psi_{\mathbf{k}}^*)$ for $\psi_{\mathbf{k}}$, which looks the same. It should be noted that

$$\Phi_{\mathbf{k}} \propto \sum_{N=0}^{\infty}\left(\frac{\psi_{\mathbf{k}}^N}{\sqrt{N!}}\right)\Phi_{\mathbf{k},N}\,,$$

where $\Phi_{\mathbf{k},N} = (1/\sqrt{N!})(p_{\mathbf{k}}^{\dagger})^N|0\rangle$ is the state with a certain number of particles N, in which the wave-function oscillation frequency is $N\omega_{\mathbf{k}}$. When various $\Phi_{\mathbf{k},N}$ are combined into a classical wave with a sufficiently large amplitude, high frequencies (responsible for quantum fluctuations) are canceled, and the observed field oscillation frequency tends to the expected average value $\omega_{\mathbf{k}}$. This frequency is solely determined by the dispersion law and, in the absence of interaction between particles, does not depend on the amplitude [6]. The problem of determining the coherent states of interacting particles is rather complicated, since it is necessary in this case to take into account the deviation of their statistics from purely bosonic, thus returning to the analysis of the multi-electron problem. This problem was considered in detail by Keldysh in study [21, 22], where a consistent 'microscopic' substantiation of the mean field approximation for exciton and exciton–photon systems has been given.

As in the case of atomic condensates and superconducting metals, the interaction between polaritons is usually considered in the dilute gas approximation, $H_{\mathrm{int}}(\mathbf{r}) = (V/2)|\psi(\mathbf{r})|^4$. If $V > 0$, pair repulsion of particles and a blue shift of the eigenfrequency arise. The shift ΔE_{LP} can significantly exceed spectral linewidth γ [76] in GaAs-based structures. As shown below, this circumstance results in strong nonlinear effects, but since the line width is only determined by the Q-factor of the cavity, it does not mean per se going beyond the low-density approximation. It is assumed in the same approximation that the interaction between particles does not destroy coherence. All basic assumptions of this kind are experimentally verified, and some cases where they may fail will be discussed separately. The case of a relatively high density of excitons is a separate area of research, the subject of which is, notably, an electron–hole liquid [77].

The coupling between polaritons is caused from a microscopic point of view by the exchange Coulomb interaction between electrons or holes; the dipole–dipole interaction at low density is negligible [78]. The assertion that polaritons with opposite spins ($J_z = \pm 1$) do not interact in pairs holds true for systems with $E_0 \lesssim E_X$ and large R, where all indirect processes involving 'dark' excitons ($J_z = \pm 2$) are turned off near the bottom of $E_{LP}(k)$ [79, 80]. However, the amplitudes ψ_+ and ψ_- can be linearly coupled due to the splitting of modes with orthogonal polarizations: for example, in the presence of a mechanical stress along one of the main crystal axes, which reduces the lattice symmetry. (For $k \neq 0$, a similar effect is created by the mirrors themselves that split the TE and TM photon modes, wherein, by definition, the electric- or magnetic-field vector is perpendicular to the plane of incidence of the wave [81].)

We arrive as a result at Enqs (1), in which the effective external electric field $f_{\pm}$ was introduced taking into account the transmittance of the mirrors (there is no magnetic field in the standing-wave antinode). If the cavity is excited in a wide range of frequencies and wave numbers, it is more correct to introduce separate equations for the photon and exciton amplitudes [82–84] to ensure that the external field is taken into account in only the photon part and the particle interaction in only the exciton part. But since we mainly consider polaritons near the bottom of $E_{LP}(k)$, model (1) is quite adequate.

There is no need in model (1) to take into account effects such as spin relaxation of excitons. The condensate can exist in an external field for an infinitely long time; however, all random deviations from a certain externally imposed state most often disappear during the 'polariton lifetime' $\tau = \hbar/\gamma$, which is much longer than $\hbar/R$, but at the same time shorter than any natural phase-relaxation time. In exploring the condensate in an external field, a dissipative oscillator is

usually considered that oscillates with the frequency $E_p/\hbar$ of the harmonic force acting on it. Anyway, this picture is self-consistent if E_p is near the $E_{LP}(\mathbf{k})$ resonance, implying that the value of $|\psi_{\mathbf{k}}|$ is large despite the low field density, and the concept of the *macroscopic* population of the forced polariton state with such energy may be employed.

3. Multistability of polariton condensate

We consider first a simplified version of system (1). Suppose that the spin components are not coupled ($g = 0$) and only one of them is excited, i.e., both the external field and the condensate are circularly polarized. The particles repel each other ($V > 0$); therefore, it is reasonable to look for spatially homogeneous solutions with $k = 0$. If $\gamma > 0$ and $t \to \infty$, they must oscillate with the external-field frequency. Having made the appropriate substitution $\psi(t) = \bar{\psi}\exp(-iE_p t/\hbar)$, we arrive at a time-independent equation for $\bar{\psi}$:

$$\left[E_p - \left(E_{LP} - i\gamma + V|\bar{\psi}|^2\right)\right]\bar{\psi} = f, \tag{7}$$

or

$$|\bar{\psi}|^2 = \frac{f^2}{\left(D - V|\bar{\psi}|^2\right)^2 + \gamma^2}, \tag{8}$$

where $D = E_p - E_{LP}(k=0)$. If $D > \sqrt{3}\gamma$ (see below), the dependence of $|\bar{\psi}|^2$ on f^2 takes the form of an S-shaped curve (see Fig. 2 in Section 4). The condensate state is thus *bistable* in a finite interval of f^2.

A similar phenomenon is known in laser physics [85, 86], but it occurs there in combination with nonlinear absorption or amplification of light, when V has an imaginary part and, ultimately, γ depends on ψ. However, in our case, only the eigenenergy depends on ψ. It is seen that $|\bar{\psi}| \propto f$ as $|\bar{\psi}| \to 0$, but if $E_p > E_{LP}$, then, as f and $|\bar{\psi}|$ increase, the shift $\Delta E_{LP} = V|\bar{\psi}|^2$ brings the condensate closer to resonance with the external field, decreasing the denominator in (8), as a result of which the response proves to be superlinear. With further increasing f, the system becomes *unstable*; one can say that the positive feedback loop between the amplitude and eigenfrequency leads to an increase in both of them even at constant f. Therefore, the lower branch of the S-shaped curve breaks off, and a jump of the field is expected at this point. Instability disappears when the detuning D is fully compensated by a shift in the eigenfrequency; all such solutions are on the upper branch. The middle branch with a negative slope only consists of unstable solutions.

Two critical points $V|\bar{\psi}|^2 = B_{1,2}$, at which jumps between the branches of stability are expected as f increases or decreases, can be easily found by solving the equation $df^2/d|\bar{\psi}|^2 = 0$, to yield [23, 27]

$$B_{1,2} = \frac{2D}{3} \mp \frac{1}{3}\sqrt{D^2 - 3\gamma^2}, \tag{9}$$

and the corresponding $f_{1,2}^2 = f^2(B_{1,2})$ are calculated using Eqn (8):

$$f_{1,2}^2 = \frac{2}{27V}\left[D^3 + 9D\gamma^2 \pm \sqrt{(D^2 - 3\gamma^2)^3}\right]. \tag{10}$$

It is seen that bistability exists for $D > \sqrt{3}\gamma$ and an arbitrarily small value of $V|\bar{\psi}|^2$ only provided that the quantity γ, which is determined by the quality factor of the cavity, is also sufficiently small, and D is comparable to it. Polariton bistability was first found in a GaAs-based structure with $\gamma \approx 0.2$ meV and $R \approx 2.8$ meV [27]. It manifests itself much more strongly in state-of-the-art samples with $\gamma \lesssim 0.05$ meV and $R \gtrsim 10$ meV, wherein the field is macroscopically coherent on both branches of stability, even at $D \gtrsim 10\gamma$ (see, e.g., [51]).

It should be noted that the transition of the condensate to the upper stability branch can be mediated by polaritons with other k not yet taken into account, as a result of which the threshold f_1 decreases. This effect is considered in Section 5. It is only important here that there are at once two branches of stable single-mode solutions in a certain interval f.

If the polarization of the external wave is not strictly circular, both spin components are excited. At $g = 0$ each of them can be described by its own S-shaped curve [28]. Therefore, there are in total four branches of stable solutions that differ significantly in intensity $I = |\bar{\psi}_+|^2 + |\bar{\psi}_-|^2$ or degree of circular polarization

$$\rho_c = \frac{|\bar{\psi}_+|^2 - |\bar{\psi}_-|^2}{|\bar{\psi}_+|^2 + |\bar{\psi}_-|^2}. \tag{11}$$

Suppose, for example, that the degree of circular polarization of the external field is x. Then, the four critical values of its intensity $|f_+|^2 + |f_-|^2$, at which jumps occur between branches, are $2f_{1,2}^2/(1 \pm x)$ [30]. The values of $f_{1,2}^2$ are taken from (10), although the correction mentioned above may be needed for f_1^2.

Jumps in the condensate amplitude and polarization at the critical points are directly visible in a light wave passed through the cavity. Their observation made it possible to verify with good accuracy the initial premises of the theory: coherence, the absence of spin relaxation, interaction of the form $|\psi|^4$, etc. It was found that the stronger the exciton–photon coupling, the structure itself being cleaner and more homogeneous, the less the deviation of the experimental results from model (1). For example, in the first experiments of this type performed around 2010 [31, 32, 87], the Rabi splitting was not so large, and polaritons were excited near the exciton level. Therefore, it was necessary to take into account long-lived dark (i.e., not interacting with light) excitons with $J_z = \pm 2$ that are created in pairs as a result of collisions of light excitons; the probability of this event is small, but, gradually accumulating, the dark excitons form an incoherent reservoir and affect the eigenfrequency E_{LP} [32, 88–91]. However, only a few years later, needed for the technology to be improved, it became possible in experiments to excite a relatively pure coherent state, and all the basic predictions of model (1) started being reproduced without unnecessary assumptions and fitting [80].

Numerical solution of Eqns (1) enables tracing the transition dynamics. Both calculations and experiments show that the characteristic switching times are usually comparable with $\hbar/\gamma$ and $\hbar/D$, i.e., the condensate really behaves like a forced oscillator. To record a time-resolved signal, pulsed rather than continuous pumping is used, but the multistability effect is well pronounced, even with pulses whose duration equals several $\tau = \hbar/\gamma$ [55–57].

Two-beam excitation is sometimes used: a continuous plane wave creates a multistable condensate, while a short pulse performs as a trigger for its transitions between the stability branches [35, 92]. The same role can be played by a fast acoustic pulse [93] that perturbs the lattice period, as well

as E_g, E_X, and E_{LP}, and eventually D on the time scale of τ (such pulses are generated by optical-acoustic transducers [94, 95]). The condensate behaves in both cases like a *multistable cell*. In the micropillar with a lateral size of only 3 μm studied in [35], the observed spin switching time was 5 ps at $\tau = 15$ ps, a value that is less than that in the fastest electronic switches. Such a size-quantized micropillar with a discrete E_{LP} spectrum is especially similar to a simple oscillator if all of its modes, except for one, lie above E_p and not excited.

Switching that develops with time was considered above, but sometimes states from different stability branches coexist in space. This happens when either the external field or the eigenenergy are inhomogeneous in the cavity plane. Although it is not possible in this case to operate with a single condensate mode, the concept of multistability helps to qualitatively explain what is happening, while numerical solutions of equations similar to (1) reproduce experimental results. For example, if the pump radiation is elliptically polarized, and its amplitude decreases with incresing distance from its center, a flat ring with high ρ_c emerges in the field distribution in the active layer, where amplified, i.e., located 'on the upper branch', is only one spin component; both components are enhanced inside this ring, and none of them outside [29, 32, 33]. The inhomogeneity in the eigenenergy distribution is usually compensated by a blue shift [96], but it can result near critical points in a strong polarization inhomogeneity of radiation [56].

Remarkable spatial effects also arise in the case of two-beam pumping, when one wave, which is plane and characterized by a certain wave number k_p, has a low intensity, while the other beam is an intense short pulse focused in a micrometer-sized region. The specific effect the second beam causes depends on k_p. If k_p is less than the inflection point $E_{LP}(k)$, it can trigger a chain of transitions to the upper stable state that occur one after another increasingly farther from the activation site, similar to signal transmission through a neuron [34, 97]. If k_p lies above the inflection point, the second beam can excite a soliton moving in the active layer without dissipation at a speed of $\sim 10^{-2}c$ (for GaAs) — this is like a separate representative of the upper stable state against the background of the lower one [98–102].

So, a variety of exciting effects develop from seeding inhomogeneities, and not all of them were mentioned here. However, we do not discuss them further but rather consider comparatively basic processes that can occur even in a completely homogeneous polariton system excited by a plane wave. It will be shown that the concept of a condensate in an external field as a kind of dissipative oscillator subject to a harmonic force is not always true. The phase, spatial, and spin symmetries of such a system can be spontaneously broken. These phenomena may be considered from a unified point of view by introducing above-condensate quasiparticles.

4. Bogolyubov quasiparticles

The problem on the spectrum of above-condensate modes was first considered by Bogolyubov in relation to superfluidity [46]. The polariton system is largely similar, because it has the same type of nonlinearity ($|\psi|^4$) as the model of cold-atom condensate. In particular, if the condensate momentum is zero, the weakly populated modes $\pm\mathbf{k}$ are linearly coupled with each other with a strength proportional to the condensate amplitude squared. This conclusion holds regardless of how the condensate emerged, whether in an equilibrium way or in an external field; therefore, the same unitary transformation results in particles with similar properties. There are, however, two significant differences between our system and the equilibrium condensate that affect the excitation spectra.

First, the frequencies of field oscillations in the condensate state are not the same; the corresponding energy is also referred to as the chemical potential, implying that this is the average energy per one particle [6]. The oscillations occur in our case at the external field frequency $E_p/\hbar$, while the equilibrium condensate oscillates at its own frequency $(E_{LP} + V|\psi|^2)/\hbar$ that is shifted due to the interaction. The energy reference point is of no importance, so E_{LP} can be subtracted, and it may be assumed that the chemical potentials in these two cases are $D = E_p - E_{LP}$ and $V|\psi|^2$, respectively. It follows from Eqn (9) that $V|\psi|^2 = D$ at the left turning point of the S-shaped curve (B_2) at $\gamma \to 0$. It is at this and only this point that the 'sound' excitation spectrum emerges, similar to the equilibrium Bose–Einstein condensate.

Second, nonequilibrium condensate can lose stability. This occurs if the excitation spectrum contains modes with the positive imaginary part of the energy that grow with time rather than attenuate in a usual manner, which results in growing fluctuations. Bogolyubov showed that instability is equivalent to a violation of thermal equilibrium and therefore contradicts the original premise of Bose condensation. Here, however, an initially nonequilibrium and, moreover, an open system is considered. An instability in a conservative system would only lead to a redistribution of energy between modes, and, in the simplest case, a growing mode itself would become one of the order parameters, taking some of the energy from the condensate [103]. However, it is sometimes difficult in our case to predict the new state to which the system will evolve as a result of the development of instability. Described below is a very simple 'soft mode' bifurcation, which, as explained in Section 5, can lead to the accumulation of condensate energy, multiple scattering, and further rearrangement of the excitation spectrum.

We use for simplicity Eqn (1) without taking into account the spin and switch to the momentum space by setting

$$\psi(\mathbf{r}, t) = \sum_{\mathbf{k}} \psi_{\mathbf{k}}(t) \exp(\mathrm{i}\mathbf{k}\mathbf{r}) . \tag{12}$$

It should be noted that the meaning of $\psi_{\mathbf{k}=0}$ coincides with that of the *local* amplitude $\bar{\psi}$ in Eqn (7), and no changes in the units are needed. We arrive at a system of equations [26, 38]

$$\mathrm{i}\hbar \frac{\mathrm{d}\psi_{\mathbf{k}}}{\mathrm{d}t} = \left(E_{LP}(\mathbf{k}) - \mathrm{i}\gamma\right)\psi_{\mathbf{k}} + \delta_{\mathbf{k},0} f \exp\left(-\frac{\mathrm{i}E_p t}{\hbar}\right) + V \sum_{\mathbf{q}_1} \sum_{\mathbf{q}_2} \psi^*_{\mathbf{q}_1+\mathbf{q}_2-\mathbf{k}} \psi_{\mathbf{q}_1} \psi_{\mathbf{q}_2} . \tag{13}$$

We now set

$$\psi_{\mathbf{k}}(t) = \delta_{\mathbf{k},0}\bar{\psi} \exp\left(-\frac{\mathrm{i}E_p t}{\hbar}\right) + \tilde{\psi}_{\mathbf{k}} \exp\left(-\frac{\mathrm{i}\tilde{E}(\mathbf{k})t}{\hbar}\right), \tag{14}$$

where $|\tilde{\psi}_{\mathbf{k}}/\bar{\psi}| \ll 1$ for all $\mathbf{k}$, $\tilde{E}(\mathbf{k})$ is the sought-for function. We assume that $\bar{\psi}$ satisfies Eqn (7); then, all the terms $\propto \exp(-\mathrm{i}E_p t/\hbar)$ in Eqn (13) for $\mathbf{k} = 0$ mutually cancel. Multiplying both sides of Eqn (13) by $\exp(\mathrm{i}\tilde{E}(\mathbf{k})t/\hbar)$, we

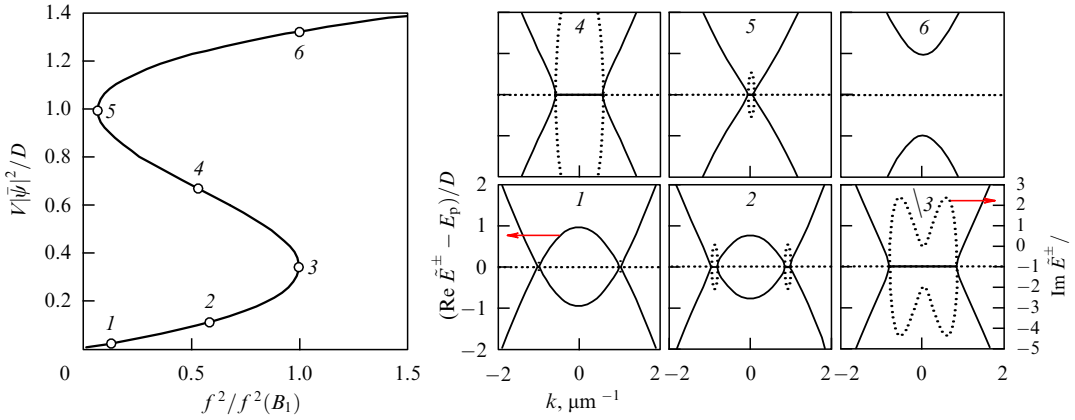

Figure 2. Spectra of the Bogolyubov quasiparticles $\tilde{E}^{\pm}(k)$ at various points of the S-shaped curve, $\gamma = 0.05$ meV, $D = 10\gamma$, and other parameters are the same as in Fig. 1.

obtain for all $\mathbf{k}$ in the first order in $\tilde{\psi}_\mathbf{k}$

$$\tilde{E}(\mathbf{k})\tilde{\psi}_\mathbf{k} = \big(E_\mathrm{LP}(\mathbf{k}) - \mathrm{i}\gamma\big)\tilde{\psi}_\mathbf{k} + 2V\bar{\psi}^*\bar{\psi}\tilde{\psi}_\mathbf{k} + V\bar{\psi}^2\tilde{\psi}^*_{-\mathbf{k}}\exp\left[-\frac{\mathrm{i}\big(2E_\mathrm{p} - \tilde{E}(\mathbf{k}) - \tilde{E}(-\mathbf{k})\big)t}{\hbar}\right]. \quad (15)$$

No terms except the last one depend on t; hence,

$$\tilde{E}(\mathbf{k}) + \tilde{E}(-\mathbf{k}) = 2E_\mathrm{p}\,. \quad (16)$$

This equation is in essence a condition of the phase balance that is needed for solutions of the form (14) to exist; it represents as well the conservation of energy in elementary scattering events $(0,0) \leftrightarrow (\mathbf{k}, -\mathbf{k})$.

As follows from Eqn (15), the condensate yields an additive correction $2V|\bar{\psi}|^2$ to the energy of any mode (the next to the last term) and, in addition, couples the $\pm\mathbf{k}$ modes (the last term), thus also affecting their energies. To formulate the problem in a closed form, the same equation for $\tilde{\psi}_{-\mathbf{k}}$ should be added, a complex conjugation made in it for all terms, and $\tilde{E}(-\mathbf{k})$ should be expressed through $\tilde{E}(\mathbf{k})$ according to (16). We arrive as a result at

$$\begin{pmatrix} a_{11} & a_{12} \\ a_{21} & a_{22} \end{pmatrix}\begin{pmatrix} \tilde{\psi}_\mathbf{k} \\ \tilde{\psi}^*_{-\mathbf{k}} \end{pmatrix} = \mathbf{0}\,, \quad (17)$$

where

$$a_{11} = E_\mathrm{LP}(\mathbf{k}) + 2V|\bar{\psi}|^2 - \mathrm{i}\gamma - \tilde{E}(\mathbf{k})\,, \qquad a_{12} = V\bar{\psi}^2\,,$$

$$a_{21} = -V\bar{\psi}^{*2}, \qquad a_{22} = 2E_\mathrm{p} - E_\mathrm{LP}(-\mathbf{k}) - 2V|\bar{\psi}|^2 - \mathrm{i}\gamma - \tilde{E}(\mathbf{k}).$$

Generally speaking, $\tilde{\psi}_{\pm\mathbf{k}}$ should be considered operators rather than numbers, since the excitations are small, but this is not essential for a linear problem. Solving the equation $\det(\cdot) = 0$, we obtain

$$\tilde{E}^{\pm}(\mathbf{k}) = E_\mathrm{p} - \mathrm{i}\gamma \pm \sqrt{\big(E_\mathrm{p} - E_\mathrm{LP}(\mathbf{k}) - 2V|\bar{\psi}|^2\big)^2 - \big(V|\bar{\psi}|^2\big)^2}\,. \quad (18)$$

Let us turn to the characteristic cases (Fig. 2). It can be seen, for example, that $\tilde{E}^-(\mathbf{k})$ coincides with $E_\mathrm{LP}(\mathbf{k}) - \mathrm{i}\gamma$ at $\bar{\psi} = 0$. We found above from general considerations that the usual Bogolyubov spectrum should be reproduced provided $V|\bar{\psi}|^2 = D$ and $\gamma \to 0$. Indeed, in this case we have

$$\tilde{E}^{\pm}(\mathbf{k}) - E_\mathrm{p} = \pm\sqrt{E'_\mathrm{LP}(\mathbf{k})\big[E'_\mathrm{LP}(\mathbf{k}) + 2D\big]}\,, \quad (19)$$

where $E'_\mathrm{LP}(\mathbf{k}) = E_\mathrm{LP}(\mathbf{k}) - E_\mathrm{LP}(0)$. If $E_\mathrm{X} = E_\mathrm{C}(0) = E_0$, the 'speed of sound' in the condensate is $c\sqrt{D/\varepsilon E_0}$.

The sound spectrum is in our case a degenerate solution at the boundary point B_2. For all $V|\bar{\psi}|^2 > B_2$, i.e., on the upper branch of the S-shaped curve, the condensate is in the center of the spectral gap, the width of which $\mathrm{Re}\,(\tilde{E}^+(0) - \tilde{E}^-(0))$ grows as $|\bar{\psi}|$ increases. Modes $\tilde{E}^{\pm}(0)$ are decaying, but they can be slightly populated by pulse excitation and then detected, both in the spectrum and in the form of the oscillations of the condensate amplitude [104, 105].

We now proceed to stability analysis. It should be noted first that if the radicand in (18) is less than zero, the real parts of $\tilde{E}^{\pm}$ coincide. Therefore, if the solution $\bar{\psi}$ is unstable, the spectral surfaces $\mathrm{Re}\,\tilde{E}^+(\mathbf{k})$ and $\mathrm{Re}\,\tilde{E}^-(\mathbf{k})$ are stuck together in a flat region with energy E_p. It follows, in particular, that solutions with a gap, when $\mathrm{Re}\,[\tilde{E}^+ - \tilde{E}^-] > 0$ for all $\mathbf{k}$, are stable, while instability is only possible for $V|\bar{\psi}|^2 < B_2$. Solving the inequality $\mathrm{Im}\tilde{E}^{\pm}(\mathbf{k};\bar{\psi}) > 0$ with respect to $\bar{\psi}$ at a given $\mathbf{k}$, we get $P_1(\mathbf{k}) < V|\bar{\psi}|^2 < P_2(\mathbf{k})$, where

$$P_{1,2}(\mathbf{k}) = \frac{2}{3}\big(E_\mathrm{p} - E_\mathrm{LP}(\mathbf{k})\big) \mp \frac{1}{3}\sqrt{\big(E_\mathrm{p} - E_\mathrm{LP}(\mathbf{k})\big)^2 - 3\gamma^2}\,. \quad (20)$$

These expressions coincide for $\mathbf{k} = 0$ with $B_{1,2}$; therefore, all solutions with a negative slope of the S-shaped curve are really unstable even in the micropillar. The condensate itself belongs in this case to the flat spectral region of the growing modes.

However, even being still 'intrinsically' stable, the condensate can start breaking up into other modes with $\mathbf{k} \neq 0$. This occurs at a very small amplitude. Noting that $\mathrm{d}P_1(\mathbf{k})/\mathrm{d}(E_\mathrm{p} - E_\mathrm{LP}(\mathbf{k})) > 0$ for $E_\mathrm{p} - E_\mathrm{LP}(\mathbf{k}) > 2\gamma$, it is easy to find that the scattering threshold is attained on the circle $E_\mathrm{LP}(|\mathbf{k}|) = E_\mathrm{p} - 2\gamma$ and is

$$P = \min_\mathbf{k} P_1(\mathbf{k}) = \gamma, \quad \text{if} \quad D > 2\gamma\,. \quad (21)$$

So, the condensate begins to break up, even on the lower branch of the S-shaped curve, the ratio of the thresholds P/B_1 being equal to $3\gamma/D$ for $\gamma \to 0$. The scattering threshold lies in the bistable region, since, on the other hand, $\lim_{\gamma\to 0} f^2(B_2)/f^2(P) = \gamma/D$.

Nothing can be said about what exactly happens when the threshold P is slightly exceeded in the framework of a theory linear in $\tilde{\psi}_\mathbf{k}$. Based on the observation that energy is conserved in any 'scattering event', and the loss of stability

at the point P is said to be *soft*, implying that $\max_{\mathbf{k}} \operatorname{Im} \tilde{E}(\mathbf{k})$ smoothly goes through zero as f and $|\bar{\psi}|$ increase, it would be natural to expect that a 'second-order phase transition' with a continuous dependence of $|\psi_{\mathbf{k}}|$ on f for each $\mathbf{k}$ occurs at this point. At least, this assumption is very often made in similar cases in laser physics [103]. However, in our case this assumption fails; actually, the break-up of the condensate into Bogolyubov pairs triggers the energy accumulation process, which is not similar to phase transitions of either the second or the first kind.

5. Regime with blowup

If the scattering threshold (21) is reached, energy is accumulated due to the positive feedback loop between the amplitudes of the condensate and scattered modes under constant external conditions [50, 51]. With a relatively small constant pumping

$$f^2 \gtrsim f^2(P) = \frac{\gamma}{V}\left[(D-\gamma)^2+\gamma^2\right] \tag{22}$$

that shifts the resonance by the value $V|\psi_0|^2 \gtrsim P = \gamma$, the system spontaneously switches to the upper stability branch, where, as usual, $V|\psi_0|^2 \gtrsim D$. The condensate amplitude increases over time hyperbolically, and the relatively long incubation period, the duration of which tends to infinity at $f \to f(P) + 0$, ends with a jump to the upper branch. Such processes, referred to as 'regimes with blowup', may occur, for example, in models based on a nonlinear Schrödinger equation with particle attraction (field self-focusing) [106, 107]. The blowup regime is due in our case to the system being open.

By accumulating energy, it is possible to excite a strong field in a microcavity even with a very high Q-factor $Q \propto 1/\gamma$ at $D > \gamma$. The problem is that, since Bragg mirrors reflect light both inside and outside, as Q increases, the entering of light into the cavity from the side of the radiation source becomes hampered. In this regard, the threshold intensity of not an effective but an actual external electromagnetic field could become too high, and a wave with such intensity would only damage the outermost reflective layer. But, since $f^2(P) \propto \gamma$ at $\gamma \to 0$, the dependence of the external-field threshold intensity on Q is significantly weakened.

We theoretically show in Section 5.1 that, rather than decreasing, the condensate amplitude actually increases in scattering; to this end, $\psi_{\mathbf{k}\neq 0}$ in the second order should be taken into account [50]. Section 5.2 illustrates how instability develops using as an example a numerical solution of Eqn (13). Section 5.3 contains experimental evidence of the blowup regime [51, 52] and a discussion of some general outcomes.

5.1 Theoretical analysis

We now take into account in Eqn (13) for $\mathbf{k} = 0$ all interaction terms that are proportional to ψ_0:

$$\mathrm{i}\hbar\frac{\mathrm{d}\psi_0}{\mathrm{d}t} = \left(E_{\mathrm{LP}}(0) - \mathrm{i}\gamma\right)\psi_0 + f\exp\left(-\frac{\mathrm{i}E_{\mathrm{p}}t}{\hbar}\right) + V\psi_0^*\psi_0\psi_0 + 2V\psi_0\sum_{\mathbf{k}\neq 0}\psi_{\mathbf{k}}^*\psi_{\mathbf{k}} + V\psi_0^*\sum_{\mathbf{k}\neq 0}\psi_{\mathbf{k}}\psi_{-\mathbf{k}}\,. \tag{23}$$

Arguing from the contrary, we assume that equilibrium has been attained in the process of scattering $(0,0) \to (\mathbf{k},-\mathbf{k})$, and, as a result, each mode $\mathbf{k}$ oscillates with a certain frequency and has a constant amplitude. We separate the phase factors:

$$\psi_{\mathbf{k}}(t) = \bar{\psi}_{\mathbf{k}}\exp\left(\mathrm{i}\phi_{\mathbf{k}}\right)\exp\left(-\frac{\mathrm{i}E(\mathbf{k})t}{\hbar}\right), \quad \text{where} \quad \bar{\psi}_{\mathbf{k}} \geqslant 0\,. \tag{24}$$

It is clear that equilibrium, in principle, is feasible only if the frequency balance $E(\mathbf{k}) + E(-\mathbf{k}) = 2E_{\mathrm{p}}$ is fulfilled. We obtain then from Eqn (23) a static equation that may be represented similarly to (8):

$$\bar{\psi}_0^2 = \frac{f^2}{(E_{\mathrm{p}} - E_\star - V\bar{\psi}_0^2)^2 + \gamma_\star^2}\,, \tag{25}$$

where the following notations are introduced:

$$E_\star = E_{\mathrm{LP}}(0) + V\sum_{\mathbf{k}\neq 0}(2\bar{\psi}_{\mathbf{k}}^2 + \bar{\psi}_{\mathbf{k}}\bar{\psi}_{-\mathbf{k}}\cos\alpha_{\mathbf{k}})\,, \tag{26}$$

$$\gamma_\star = \gamma + V\sum_{\mathbf{k}\neq 0}\bar{\psi}_{\mathbf{k}}\bar{\psi}_{-\mathbf{k}}\sin\alpha_{\mathbf{k}}\,, \tag{27}$$

$$\alpha_{\mathbf{k}} = 2\phi_0 - \phi_{\mathbf{k}} - \phi_{-\mathbf{k}}\,. \tag{28}$$

$E_\star$ and $\gamma_\star$ perform here as condensate eigenenergy and decay rate. If equilibrium actually exists between the condensate and all the modes into which it scatters, then an increase in the condensate decay rate at a constant value of f should result in a decrease in its amplitude,

$$\frac{\delta\bar{\psi}_0}{\delta\gamma_\star} < 0\,, \tag{29}$$

whereas, otherwise, the total energy can increase spontaneously. The symbol δ here denotes small virtual changes that are needed to analyze the stability of the static solution. We now verify relation (29). Differentiating Eqn (25), we find

$$\delta\bar{\psi}_0 = \bar{\psi}_0\frac{\delta X}{Y}\,, \tag{30}$$

where

$$\delta X = (E_{\mathrm{p}} - E_\star - V\bar{\psi}_0^2)\delta E_\star - \gamma_\star\delta\gamma_\star\,, \tag{31}$$

$$Y = (E_{\mathrm{p}} - E_\star - 2V\bar{\psi}_0^2)^2 - (V\bar{\psi}_0^2)^2 + \gamma_\star^2\,. \tag{32}$$

Using formula (25), it is also easy to verify that $Y = \partial(f^2)/\partial(\bar{\psi}_0^2)$. As $\bar{\psi}_0$ increases, this quantity changes its sign at the already known boundary point

$$V\bar{\psi}_0^2 = \frac{2}{3}(E_{\mathrm{p}} - E_\star) - \frac{1}{3}\sqrt{(E_{\mathrm{p}} - E_\star)^2 - 3\gamma_\star^2}\,, \tag{33}$$

where an amplitude jump is expected. Of interest to us is the issue of whether equilibrium can be established before the jump, so we find the minimum of $\delta X/\delta\gamma_\star$ on the lower branch of solutions. Since expression (31) decreases with increasing $V\bar{\psi}_0^2$ at $\delta E_\star > 0$, we substitute the boundary value (33) into it, yielding

$$\delta X > \frac{1}{3}\left[E_{\mathrm{p}} - E_\star + \sqrt{(E_{\mathrm{p}} - E_\star)^2 - 3\gamma_\star^2}\right]\delta E_\star - \gamma_\star\delta\gamma_\star\,. \tag{34}$$

The expression on the right-hand side of (34) decreases as both $E_\star$ and $\gamma_\star$ increase. Up to the limit point $E_{\mathrm{p}} - E_\star = \sqrt{3}\gamma_\star$, i.e., when the lower branch of solutions still exists as such, we have

$$\frac{1}{\gamma_\star}\frac{\delta X}{\delta\gamma_\star} > \frac{1}{\sqrt{3}}\frac{\delta E_\star}{\delta\gamma_\star} - 1\,. \tag{35}$$

We now find $\delta E_\star/\delta\gamma_\star$ at $\delta\bar{\psi}_{\mathbf{k}\neq 0} \geqslant 0$. The problem has circular symmetry, therefore

$$\frac{\delta E_\star}{\delta\gamma_\star} = \frac{\sum_{\mathbf{k}\neq 0} u_{\mathbf{k}}\delta v_{\mathbf{k}}}{\sum_{\mathbf{k}\neq 0}\delta v_{\mathbf{k}}}\,, \tag{36}$$

where

$$u_{\mathbf{k}} = \frac{2+\cos\alpha_{\mathbf{k}}}{\sin\alpha_{\mathbf{k}}}\,, \qquad \delta v_{\mathbf{k}} = \sin(\alpha_{\mathbf{k}})\bar{\psi}_{\mathbf{k}}\delta\bar{\psi}_{\mathbf{k}}\,. \tag{37}$$

(According to [50], the same expressions are also obtained in a more general case of a condensate with nonzero $\mathbf{k}$.) It should be noted that, if $\bar{\psi}_{\mathbf{k}} > 0$, then, under equilibrium conditions, there must be $\sin\alpha_{\mathbf{k}} > 0$, since the sign of $\sin\alpha_{\mathbf{k}}$ determines in which direction the process $(0,0) \leftrightarrow (\mathbf{k},-\mathbf{k})$ is evolving (compare with (27)). Equation (36) then has the meaning of the average value of $|u_{\mathbf{k}}|$ with the weight function $|\delta v_{\mathbf{k}}|$; therefore,

$$\frac{\delta E_\star}{\delta\gamma_\star} \geqslant \min_{\alpha}\left|\frac{2+\cos\alpha}{\sin\alpha}\right| = \sqrt{3}\,. \tag{38}$$

Combining this result with (35) and then with (30), we find out that the equilibrium condition (29) is impossible on the lower branch of static solutions.

Returning to the scattering process, we can conclude that the condensate amplitude is not bounded because of increasing losses above the threshold — on the contrary, it increases itself and, as shown in [50], the *growth rate* of the scattered modes also continuously increases in this connection. The positive feedback loop between the amplitude and the effective resonant frequency of the condensate now is mediated by the scattered modes — at first arbitrarily slowly at $f \to f(P) + 0$. However, over time, it short-circuits at the point $Y = 0$, and then a jump to the upper stability branch occurs.

The conservative nature of the $|\psi|^4$ coupling is manifested in the balance of frequencies (16), but not in the energy balance, because an external field is effective all the time. However, precisely when $\gamma \to 0$ and, in accordance with (22), $f(P) \to 0$, i.e., when the system is getting closer to being dissipativeless and conservative, this behavior is especially counterintuitive.

5.2 Numerical example

We return now to Eqns (13) and use their numerical solution as an example to shed light on the remaining problems: on the one hand, the role of fluctuations and initial conditions, and on the other hand, strong instability immediately before the jump in the condensate amplitude.

This example, taken from [50] (Fig. 3), was obtained for $D/\gamma = 12.5$ and such f^2 for which

$$f^2(P) : f^2 : f^2(B_1) \approx 1 : 1.1 : 3\,. \tag{39}$$

To simulate fluctuations, a stochastic source $\xi_{\mathbf{k}}$ is added to the right side of Eqns (13). Its phase $\arg\xi_{\mathbf{k}}$ is a random variable uniformly distributed from 0 to 2π, which is updated every 0.08 ps ($\lesssim \hbar/R$) at each node of the computational mesh $\mathbf{k}$. The amplitude $|\xi_{\mathbf{k}}|$, which is constant and the same for all $\mathbf{k}$, is chosen in such a way that for $f = 0$ the average population of each mode is $V|\psi_{\mathbf{k}}|^2 \sim 10^{-9}P$. The dispersion law $E_{\mathrm{LP}}(k)$ is determined by the parameters $E_{\mathrm{C}}(0) = E_{\mathrm{X}} = 1.45$ eV, $R = 6.4$ meV, and $\varepsilon = 12.5$. The resonance width is

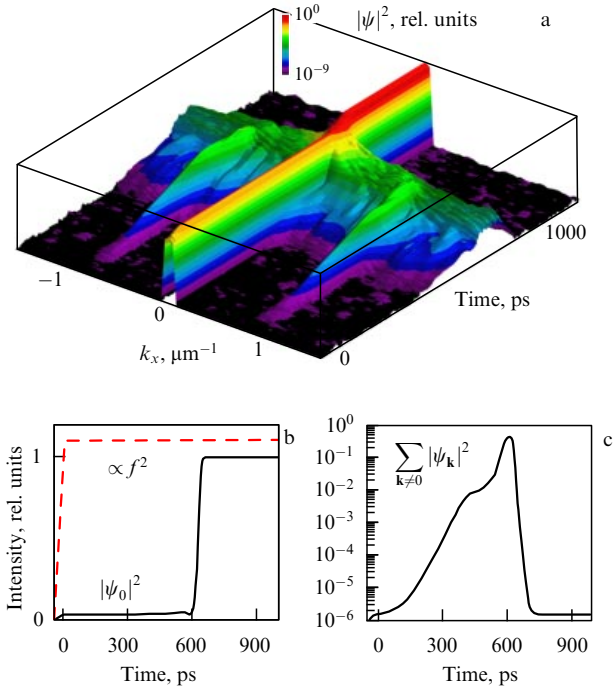

Figure 3. (Color online.) Polariton system evolution in the blowup regime [50]. (a) Distribution of $|\psi_{\mathbf{k}}(t)|^2$ along the $k_y = 0$ axis. (b) Intensities of the pump and condensate mode; (c) total intensity of all above-condensate modes as a function of time.

$\gamma = \hbar/\tau = 0.04$ meV ($\tau \approx 16$ ps), the pump detuning $D = 0.5$ meV, the wave number range is $-1.5 \leqslant k_{x,y} \leqslant 1.5$ μm^{-1}, the mesh size is 81×81, and the boundary conditions are periodic. In 50 ps, pump f^2 linearly increases from zero to level (39), and then remains constant. The moment at which f^2 attains a given level is taken as zero on the timeline. We are interested in the subsequent evolution of the system, which does not depend on the specific value of the constant V taken into account in the definitions of $f^2(B_1)$ (see (10)) and $f^2(P)$ (see (22)). To integrate the equations, the variable-step Runge–Kutta method was used.

According to (13), the quantity $|\psi_{\mathbf{k}}|$ is proportional to $|\psi^*_{-\mathbf{k}}|$. Consequently, in an ideal system, the condensate does not break up if $\psi_{\mathbf{k}} = 0$ for all $\mathbf{k} \neq 0$. Nonzero $\psi_{\mathbf{k}}$ are easily provided by Rayleigh scattering, but it also prevents the nonlinear signal from growing against the noise background. The emergence of correlated signal/idler pairs from a noise substrate is a complex process, the duration of which depends on the relation between the characteristic signal growth times $\hbar/\operatorname{Im}\tilde{E}(\mathbf{k}, |\bar{\psi}_0|)$ and its random dephasing. Our consideration is restricted by an illustration: as follows from Fig. 3, regular growth $|\psi_{\mathbf{k}}(t)| \propto \exp(\Gamma t)$ with constant Γ starts only at $t \approx 160$ ps $\approx 10\,\tau$. By the time it ends ($t \approx 400$ ps), a slight increase in $|\psi_0|$ becomes noticeable.

After $t \approx 400$ ps, a new disorder sets in which is now of a purely dynamic nature. The condensate is now turns out to be at the center of a large circle of growing modes ($\operatorname{Re}\tilde{E}^{\pm}(\mathbf{k}) = E_{\mathrm{p}}$) with various $|\mathbf{k}|$. Secondary scattering channels emerge that are not taken into account in Eqn (23), and the system loses the phase distribution $\alpha_{\mathbf{k}}$ at which the energy was accumulated earlier. However, the condensate is itself unstable; at some moment in time, it abruptly changes the phase, increases the amplitude, and, having reached the upper stability branch, no longer breaks up ($t \gtrsim 600$ ps).

The duration of the individual stages of this transition can be changed depending on the choice of the parameters, but if the system is homogeneous and the energy cannot leave it otherwise than being radiated out of the cavity, the stage of the exponential growth of the scattered modes inevitably ends up with a jump to the upper stability branch.

5.3 Experiments

The blowup regime was observed in the process of pulsed pumping [51], when the values of $|\psi_{\mathbf{k}}(t)|^2$ could be measured directly (with an accuracy to the transmittance factor). The pulse in [51] had a Gaussian shape with a lateral size of 45 μm and a duration of about 200 ps. It was shown that the onset of scattering actually triggers the energy accumulation process. The population of scattered modes were found to increase even with decreasing pump, i.e., at the back front of the pulse, and the jump in $|\psi_0|^2$ was then observed when $f^2(t)$ was halved with a delay of about 100 ps relative to the maximum. Moreover, in full accordance with Fig. 3, modes with a certain $|\mathbf{k}|$ were excited in the beginning of the transition, which was followed by the excitation of a wide region around the condensate. As expected, the blowup regime was absent when pumping was too weak or too strong.

A question arises: is it possible to somehow retain the evolution of the system in its most unstable phase? To do so, it is necessary to ensure the outflow of energy without breaking the feedback loop between the condensate and scattered modes. It turns out to be possible provided a small spot several micrometers in radius is only excited in a normal laterally homogeneous structure [52]. In this setup, polaritons with nonzero $\mathbf{k}$ that move out constantly take away some energy outside the unstable region in the center of the spot.

Experiment [52] was performed with continuous pumping. Typical of this setup, the transmission signal was not resolved in time, but could be accumulated for an arbitrarily long time near the threshold. As the external-field amplitude increased, two signal jumps were observed: the first corresponded to the overcoming of the Rayleigh signal by growing scattered mode, and the second to the transition to the upper stability branch. In between, the transition remains incomplete even at $t \to \infty$ because of the energy outflow. It is clear that instability is strongest immediately before the second jump. The condensate experiences here a strong feedback effect of scattered modes, whose amplitudes are small on average, but vary rapidly and randomly. Consequently, all modes, including the condensate itself, no longer resemble an oscillator excited by a constant harmonic force, so the assumption of macroscopic coherence may fail. Indeed, it was in this and only this region that the second-order time correlation function measured using a Brown–Twiss interferometer showed a jump to 1.8 instead of the value of 1.0 typical of classical light.

In handling *nonclassical* polariton states that arise from scattering, Josephson junctions, etc., it is usually assumed that at least one of the coupled modes has a low population that allows quantum effects to manifest themselves [108–110]. By contrast, in our case the incoherent states are, in a sense, brought about solely by the condensate. The super-Poisson statistics of photons emerged when the field intensity was already an order of magnitude greater than in an apparently coherent state below the threshold. Moreover, as early as 2004, nonclassical radiation with a 'squeezed' uncertainty relation was reported in the run-up to the transition to the upper branch, but the effect was not very large in a homogeneous polariton system [111].

Another noteworthy effect found in Ref. [52] is the spontaneous breaking of circular symmetry. Inhomogeneities in the distribution of unstable scattered modes arise and get amplified so that they compete with each other, suppress the nearest neighbors, etc. A symmetric Gaussian spot transforms as a result into a regular polygon. The orientation and the number of its sides are apparently determined by the small inhomogeneity of the sample itself, since they depend in the experiment on the location of the pump spot. This effect was observed in a wider range of amplitudes than radiation with quantum noise. Thus, the introduction of lateral heterogeneity results in interesting new phenomena in a polariton system with multimode instability.

6. Break-up of a condensate with nonzero momentum

6.1 Parametric scattering

Let us consider an effect that at the turn of 2000 caused the first surge of interest in the collective states of polaritons in a microcavity. This is the break-up of a condensate excited with a wave number k_p near the inflection point of the lower polariton branch, as a result of which new coherent modes with wave numbers 0 and $2k_\mathrm{p}$ emerge. The inflection point is also referred to as the 'magic angle', since the condensate wave number is controlled in the general case by the angle of incidence of light: $k_\mathrm{p} \approx [E_0/(\hbar c)] \sin\theta$, yielding $\theta \approx 15^\circ$ at the $E_\mathrm{LP}(k)$ inflection point for GaAs with $E_0 = E_\mathrm{C}(0) = E_\mathrm{X}$.

Scattering from condensate was initially detected in the 'parametric amplifier' mode by measuring the transmittance of the second beam with the wave number $k = 0$ and a relatively small amplitude [112, 113]. It became clear shortly after that the second beam is not needed, and the condensate can break-up fully spontaneously [36, 114, 115]. Such a break-up was explained in [116, 117] by analogy with an optical parametric oscillator (OPO), in which the 'pump' beam is split into a half-frequency 'signal' and 'idler'. It is for this reason that the same terms are sometimes still used to label unstable Bogolyubov modes that also emerge in pairs. However, the nonlinear term in the equations of evolution of a conventional OPO is of the second degree in the amplitude, while in our case it is of the third degree. If we take only three equations from a system like (13) for $\mathbf{k} = 0$ (signal), $\mathbf{k}_\mathrm{p}$ (condensate excited by an external field), and $2\mathbf{k}_\mathrm{p}$ (idler), then we can easily determine the relationship between the signal and condensate amplitudes above the scattering threshold, which turns out to be the same as in experiment [37]: $|\psi_0| \propto |\psi_{\mathbf{k}_\mathrm{p}}|^2$.

The question to be answered then is: why does the signal prefer to emerge in the $\mathbf{k} = 0$ state? The same experiments [37] showed that there is nothing *magic* in the inflection point, and the condensate can break up at various θ varying from 10° to 24°, while the signal only shifts upward in frequency as θ increases but does not change its wave number. The calculation of the Bogolyubov spectra did not clarify the situation. To generalize the results of Section 4 for the case $\mathbf{k}_\mathrm{p} \neq 0$, we should make the substitution $-\mathbf{k} \to 2\mathbf{k}_\mathrm{p} - \mathbf{k}$ in each of Eqns (15)–(17). This yields a slightly more complex expression for $\tilde{E}^{\pm}(\mathbf{k})$, but the blue shift $V|\psi_{\mathbf{k}_\mathrm{p}}|^2$ at the threshold point is still equal to γ. For small γ, the dispersion surfaces $\mathrm{Re}\,\tilde{E}^{\pm}(\mathbf{k})$ are almost unperturbed, and the scattering

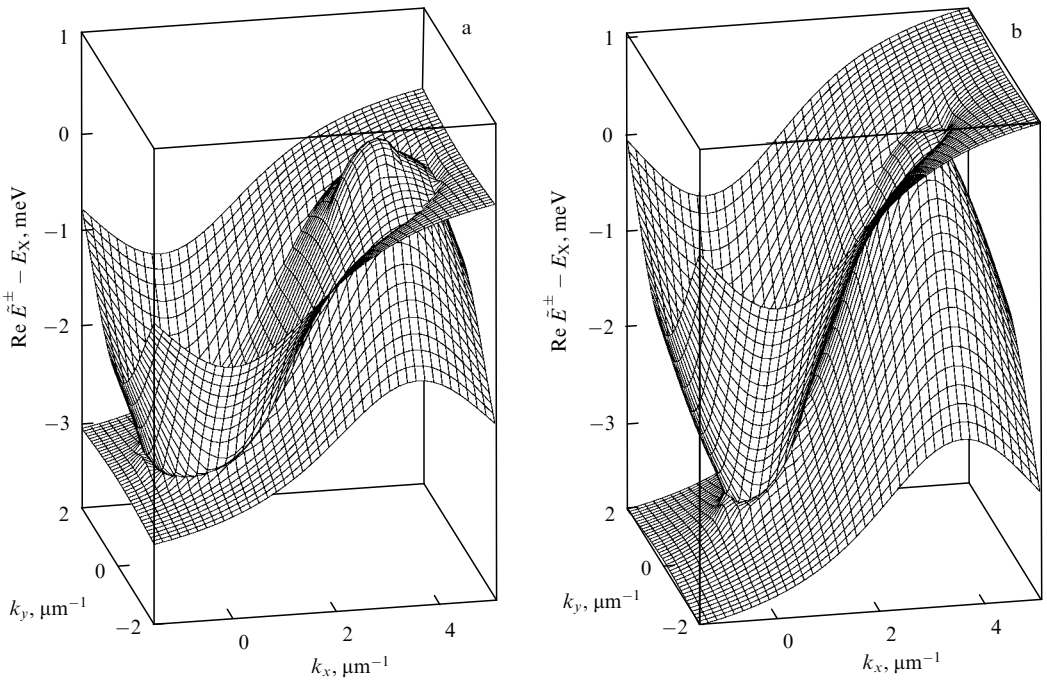

Figure 4. Distribution $E = \mathrm{Re}\,\tilde{E}^{\pm}(k_x, k_y)$: (a) on the lower branch of the S-shaped curve at $f \lesssim f(B_1)$; (b) on the upper branch with the same f. Parameters: $R = 6.4$ meV, $\mathbf{k}_\mathrm{p} = (1.8, 0)$ μm^{-1}, $D \approx 0.5$ meV $\approx 3\gamma$ (from article [43]).

directions are determined immediately from the phase balance condition similar to (16):

$$E_{\mathrm{LP}}(\mathbf{k}) + E_{\mathrm{LP}}(2\mathbf{k}_\mathrm{p} - \mathbf{k}) = 2E_\mathrm{p}\,. \tag{40}$$

The pump frequency E_p slightly exceeded in the experiments the resonant frequency $E_{\mathrm{LP}}(\mathbf{k}_\mathrm{p})$, since due to this the signal was enhanced. Provided that $D > 0$, all points (k_x, k_y) lie on a circle when $\mathbf{k}_\mathrm{p} = 0$; if, however, $\mathbf{k}_\mathrm{p}$ is near the magic angle, they lie on a kind of ∞ symbol with wide loops around $\mathbf{k} = 0$ and $2\mathbf{k}_\mathrm{p}$ open at the center point $\mathbf{k}_\mathrm{p}$.

It was assumed at first in [38] that, for the $\mathbf{k} = 0$ signal mode to be macroscopically populated, other scattering channels are needed that were not taken into account in (1) and (13), which, for example, could deteriorate the stability of all *nonground* states with higher eigenenergies. Another explanation was suggested by N A Gippius and S G Tikhodeev [26, 39, 83, 118], who noted that the condensate must be bistable in the case of a positive detuning D. It is on the upper branch of solutions that the dispersion surfaces $\mathrm{Re}\,\tilde{E}^{\pm}(\mathbf{k})$ are stuck together near $\mathbf{k} = 0$ and $2\mathbf{k}_\mathrm{p}$ almost independently of the specific $\mathbf{k}_\mathrm{p}$, because the $\mathrm{Re}\,\tilde{E}^{+}(\mathbf{k})$ surface is strongly shifted to the blue part of the spectrum, while $\mathrm{Re}\,\tilde{E}^{-}(\mathbf{k})$ to the red part (Fig. 4) They touch each other at the points close to 0 and $2\mathbf{k}_\mathrm{p}$ at the largest amplitude at which scattering is still possible. But the upper branch can only be reached after a jump in the amplitude; therefore, the phase transition that occurs is not of the second kind, as was previously assumed by analogy with the OPO [37], but rather of the first kind. Experiments with pulsed pumping and time resolution, which were performed several years later [42, 119, 120], clearly showed a rapid enhancement of both the condensate and the signals upon reaching the threshold. A sharp transition from distribution (40) to a giant signal with zero $\mathbf{k}$ was detected around the same time in a series of experiments with various constant f, a phenomenon that would have been impossible without a jump in $|\psi_{\mathbf{k}_\mathrm{p}}|$ [43]. It was found even earlier that the signal and the idler feature high spatiotemporal coherence [41].

The scenario that suggested a jump in amplitude at the beginning of the entire process also encountered an obvious difficulty: as D/γ increases, the threshold f_1 of the transition between the lower and upper branches of the response significantly exceeds the scattering threshold. At first, this inconsistency was again explained by effects unaccounted for, for example, fluctuations that can actually lower f_1 [121–125]; however, the 'soft' parametric scattering expected for $D > 2\gamma$ was not observed, even in very high-quality samples at low temperature. The whole picture was only pieced together with account taken of the feedback loop between the condensate and signals, i.e., the blowup regime, which well explains the details of previous experiments [50]. The primary nonlinear effect is precisely parametric scattering, but, by exciting the signals, the condensate enhances itself and shifts the $\mathrm{Re}\,\tilde{E}^{\pm}(\mathbf{k})$ surfaces in opposite directions, due to which the distribution of scattering directions changes all the time. As a result of an increase in energy, the loops get closed around the points 0 and $2\mathbf{k}_\mathrm{p}$, and the condensate enters the spectral gap and then actually breaks up, transferring excess energy to the signal modes. Both loops and bistability eventually degenerate in full ($E_\mathrm{p} - E_\star < \sqrt{3}\gamma_\star$). Therefore, it turns out in experiments with continuous pumping that the signal, which, at first glance, should emerge smoothly, experiences a giant jump, while the bistable condensate, on the contrary, barely changes its amplitude.

Equations (1) with an external field $\propto \exp[\mathrm{i}(\mathbf{k}_\mathrm{p}\mathbf{r} - E_\mathrm{p}t/\hbar)]$ gradually lose their relevance as $\mathbf{k}_\mathrm{p}$ is shifted to the exciton region ($\theta \gtrsim 40^\circ$), where incoherent scattering comes into play [126, 127]. If $\mathbf{k}_\mathrm{p}$ is shifted in the reverse direction from the magic angle to zero, the pair $(0, 2\mathbf{k}_\mathrm{p})$ ceases to play a special role, and, moreover, interference from the Rayleigh signal near the threshold gets stronger. The blowup regime becomes a purely transient effect in the vicinity of $\mathbf{k}_\mathrm{p} = 0$, as described for simplicity in Section 5.

6.2 Rayleigh scattering and superfluidity

A modification of the Bogolyubov spectrum is associated with another remarkable threshold effect: a transition to 'superfluid' behavior where elastic Rayleigh scattering of polaritons on structural inhomogeneities is turned off [13, 47, 48].

Figure 5 shows solutions to system (13) with a 'defective' micrometer-sized region where the eigenenergy is anomalously large. Polaritons excited with a nonzero wave number k_p are scattered on such a defect. For example, interference of the condensate and a circular wave spreading in the backward direction is visible in Fig. 5b, f. Many modes are populated in the momentum space, even without taking into account nonlinearity, the frequency of any mode with a nonzero average $|\psi_{\mathbf{k}}|$ being equal to the condensate frequency $E_p/\hbar$ and, therefore, $\mathbf{k}$ satisfying the condition

$$\operatorname{Re}\tilde{E}^{\pm}(\mathbf{k}) = E_p \qquad (41)$$

for at least one of the branches $\tilde{E}^{\pm}$. On the other hand, parametric scattering not related to nonhomogeneity is determined by the condition $\operatorname{Im}\tilde{E}^{\pm}(\mathbf{k}) > 0$, or

$$\operatorname{Re}\tilde{E}^{+}(\mathbf{k}) = \operatorname{Re}\tilde{E}^{-}(\mathbf{k})\,. \qquad (42)$$

The roots of Eqns (41) and (42) depend on the position and amplitude $\bar{\psi}$ of the condensate mode.

All calculations, the results of which are displayed in Fig. 5, are performed at $D = 2\gamma = 0.1$ meV. The solution plotted in Fig. 5a, b lies on the lower branch of the S-shaped curve, while two other solutions (Fig. 5c, d and 5e, f) lie on the upper one, and they are outside the bistable region. Thus, all the spectra in Fig. 5a, c, e are directly attainable when the pump is switched on smoothly from zero to the required amplitude f. With the exception of this circumstance, Fig. 5c corresponds to state *5* in Fig. 2, in which the condensate with zero k_p also has a sound excitation spectrum.

As can be seen from a comparison of Fig. 5a and c, all the roots of Eqns (41) and (42) degenerate into the point $\mathbf{k} = \mathbf{k}_p$ as $|\bar{\psi}|$ increases and then completely vanish. Then, since all ways of polariton scattering are closed, their motion becomes superfluid, and the scale of the inhomogeneity no longer exceeds the defect size (Fig. 5d).

The situation in which both scattering paths disappear almost simultaneously as $|\bar{\psi}|$ increases is only typical of relatively small k_p. For larger k_p, the parametric break-up of the condensate ceases earlier than Rayleigh scattering, as can be seen from Fig. 5e. In addition, the field distribution around the defect changes (Fig. 5f). The motion of the defect relative to polaritons becomes *supersonic* when the speed of motion $\hbar k_p/m_{LP}$ is higher than the speed of sound in condensate $[\mathrm{d}(\operatorname{Re}\tilde{E})/\mathrm{d}(\hbar k)]_{k\to k_p}$. These speeds do not have an exact meaning for the system as a whole; nevertheless, the supersonic effect is noticeable owing to the V-shaped feature in the $|\psi|^2$ distribution that corresponds to the Mach cone [128].

The transition to superfluidity under the conditions of resonant pumping is not very similar to the behavior of real liquids and gases if threshold phenomena like a jump in heat capacity, which usually accompany such transitions, are meant. As was asserted above, polaritons in an external field have neither critical temperature nor equilibrium in general, and the transition conditions are different. For example, the state displayed in Fig. 5e, f become superfluid if the external field is slightly enhanced so that the $\operatorname{Re}\tilde{E}^{\pm}(\mathbf{k})$ branches move apart (as in state *6* in Fig. 2) and condition (41) becomes impossible for all $\mathbf{k}$. Thus, superfluidity emerges as $\bar{\psi}$ increases; however, this transition per se may look different due to possible bistability of the response.

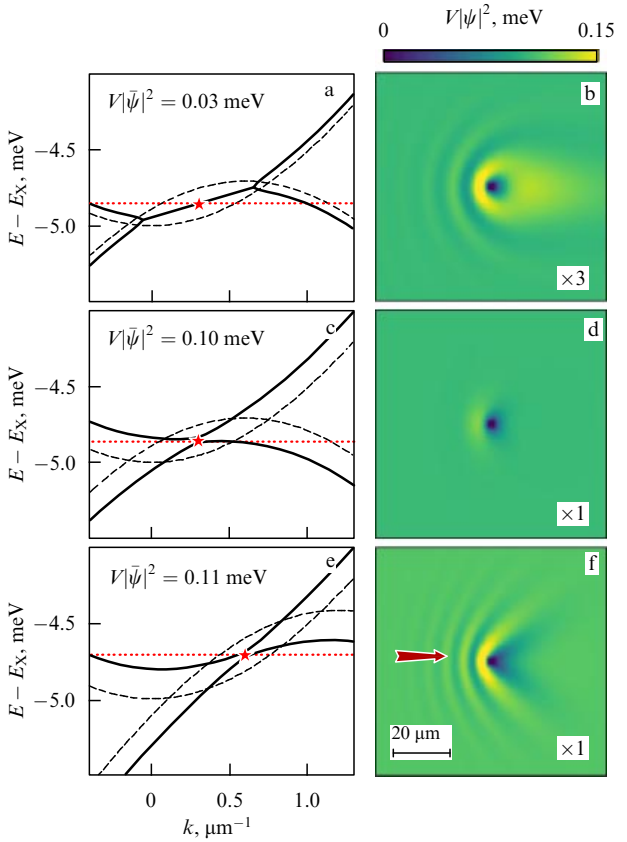

Figure 5. (Color online.) Illustration of transitions to (a–d) superfluidity and (e, f) supersonic motion. Spectra (a, c, e) of the Bogolyubov modes $\operatorname{Re}\tilde{E}^{\pm}(k)$ (solid curves). The pump position (k_p, E_p) is marked by a star; the condensate mode 'intensity' $V|\bar{\psi}|^2$ is shown explicitly in each case; the dashed curves show the undisturbed dispersion law $E_{LP}(k)$ and its 'idle' replica $2E_p - E_{LP}(2k_p - k)$; the dotted line shows the pump level $E = E_p$. (b, d, f) Corresponding numerical solutions of Eqns (13) that have established with time. The pump acts in the direction of the arrow. In the center of the computational mesh, there is a 'defect' 1 μm in radius, inside which the eigenenergy E_{LP} for all $\mathbf{k}$ is several meV higher than the usual value. Cavity parameters correspond to Fig. 1; the decay rate $\gamma = 0.05$ meV.

The superfluidity effect in a nonequilibrium polariton condensate predicted in [47] was confirmed experimentally, as was supersonic motion [48]. Both effects have been recently observed even at room temperature in a cavity with an active layer made of organic material, in which the Rabi splitting was as high as 0.6 eV [49]. These experiments have shown that the system actually does not have different break-up channels or excitation carriers other than Bogolyubov particles to which the condensate energy can be transferred. Thus, they confirm the self-consistency of the theory.

7. Spin symmetry breaking

The autonomous Gross–Pitaevskii or Ginzburg–Landau equations are invariant with respect to the phase shift $\psi \mapsto \psi \exp(\mathrm{i}\phi)$; therefore, the equilibrium Bose condensate always emerges spontaneously, breaking the continuous gauge symmetry U(1) [6]. The condensate phase in a strong external field, as a rule, is predetermined by this field;

however, Bogolyubov particles originate in pairs and are characterized by a certain value of $\alpha_{\mathbf{k}} = 2\phi_{\mathbf{k}_p} - \phi_{\mathbf{k}} - \phi_{2\mathbf{k}_p-\mathbf{k}}$, whereas the phases themselves are randomly selected. Thus, pairwise break-up of the condensate is also related to the breaking of the U(1) symmetry.

We begin here to describe a new scattering mechanism, due to which, not a pair, but a continuum of polariton modes with various $|\mathbf{k}|$ can be excited at constant f and without any structural defects whatsoever. The primary nonlinear effect in this mechanism is violation of parity, i.e., the spin balance at $f_+ = f_-$ [55–57, 129–131]. We analyze this phenomenon in this section to show in Section 8 how and under what conditions it can result in a violation of continuous symmetry. All the issues that we discuss are contained in Eqns (1) that describe a homogeneous system under the effect of a plane light wave ($\mathbf{k}_p = 0$).

7.1 Theoretical analysis

Having made the substitution $\psi_\pm(t) = \bar{\psi}_\pm \exp(-iE_p t/\hbar)$, we obtain

$$\left(D + i\gamma - V|\bar{\psi}_\pm|^2\right)\bar{\psi}_\pm - \frac{g}{2}\,\bar{\psi}_\mp = f_\pm\,. \tag{43}$$

Let $f_+ = f_- = f$, so that the light is linearly polarized in the x direction according to the usual rule $f_\pm = (f_x \mp i f_y)/\sqrt{2}$. System (1) can be diagonalized at $\psi_\pm \to 0$ if $\psi_\pm$ is expressed through $\psi_{x,y}$ in the same way; two eigenenergies $E_{x,y}$ are equal to $E_{LP} \pm g/2$. Therefore, the incident light is polarized in the same way as the upper (lower) eigensublevel at $g > 0$ ($g < 0$). Excluding f from (43), we obtain

$$\frac{\bar{\psi}_-}{\bar{\psi}_+} = \frac{D + g/2 + i\gamma - V|\bar{\psi}_+|^2}{D + g/2 + i\gamma - V|\bar{\psi}_-|^2}\,. \tag{44}$$

It can be seen that, along with spin-symmetric solutions ($\bar{\psi}_+ = \bar{\psi}_-$), which are always present, there are also asymmetric solutions, where one of the spin components is smaller than the other and completely vanishes at $\gamma \to 0$ and some f. For example, $\lim\limits_{\gamma\to 0} \bar{\psi}_- \propto \gamma$ if

$$V|\bar{\psi}_+|^2 = D + \frac{g}{2}\,. \tag{45}$$

If $g > 0$, symmetric solutions may be unattainable in finite regions of f and D (Fig. 6). To make it clear, notice that the strength with which one component acts on the other depends on the difference between their phases. A similar circumstance results in the Josephson effect in tunnel-coupled superconductors [132] or Bose condensates [133–136], including polariton ones [14, 15, 137–140]. In our case, when there is an external field, the phases $\phi_\pm$ are initially the same, but they depend on the amplitude. It is already seen from Eqn (7) that as the amplitude increases the condensate phase lags behind that of the external field: $\phi \equiv \arg(f^*\psi)$ decreases from 0 at $\gamma \to 0$ and $|\psi| \to 0$ to $-\pi$ at $|\psi| \to \infty$. This conclusion is valid for both components, and if, for example, $|\psi_+| > |\psi_-|$, then, for self-consistency, there should be $0 < \phi_- - \phi_+ < \pi$, and therefore, $\sin(\phi_- - \phi_+) > 0$. On the other hand, in accordance with (1),

$$\frac{d|\psi_\pm|}{dt} = \frac{g}{2\hbar}|\psi_\mp| \sin(\phi_\mp - \phi_\pm) + \ldots\,. \tag{46}$$

If $g > 0$, the larger of the spin components, whether ψ_+ or ψ_-, is additionally enhanced at the expense of the smaller one and suppresses it. It is for this reason that spin-symmetric solutions with large amplitudes $\psi_+ = \psi_-$ are sometimes difficult to attain or simply unstable. When both components grow in the blowup regime, they compete with each other, and the component that incidentally lags behind the other can be eventually heavily suppressed.

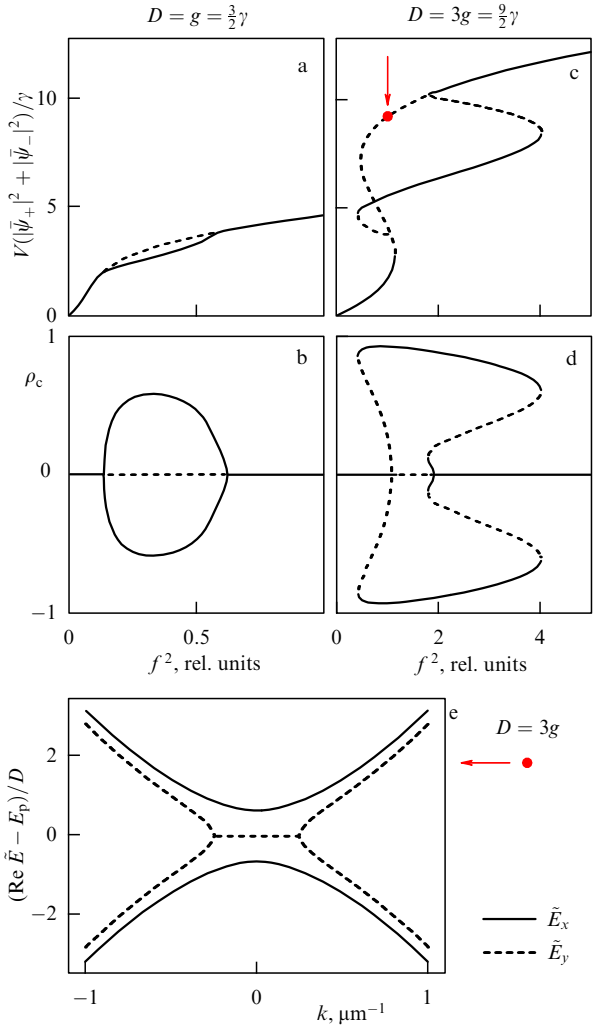

Figure 6. Solutions of Eqns (43) for $\gamma = 0.05$ meV, $g = (3/2)\gamma$, (a, b) $D = g$, and (c, d) $D = 3g$. Figures a, c show the total intensity; Figs b, d display the degree of circular polarization (11). The dashed curves show the solutions that are unstable even without the modes $k \neq 0$ being taken into account. (e) The excitation spectrum for the selected solution that is indicated by the arrow. If $\bar{\psi}_+ = \bar{\psi}_-$, all above-condensate modes are polarized in the x or y direction; their energies $\mathrm{Re}\,\tilde{E}_{x,y}$ are shown by solid and dashed curves, respectively. The cavity parameters are the same as in Fig. 1.

The evolution of the system depends on the relation between g and γ. For $0 \lesssim g \lesssim \gamma$, both symmetric and asymmetric solutions of Eqns (43) exist and are stable in a wide range of f and D. The specific state to which the system will switch may depend on the pulse shape (f as a function of t). However, as g increases to γ or higher, the internal antagonism between the spin components also enhances and, for $D \sim g$, an interval of f emerges in which all symmetric solutions altogether are unstable. (In particular, on the very top branch of solutions, where $\bar{\psi}_+ = \bar{\psi}_-$, and hence $\bar{\psi}_y = 0$, it turns out that $\mathrm{Im}\,\tilde{E}_y > 0$ for above-condensate modes.) Spontaneous symmetry breaking is inevitable in this range of f, regardless of the pulse shape, lateral size of the system, etc.

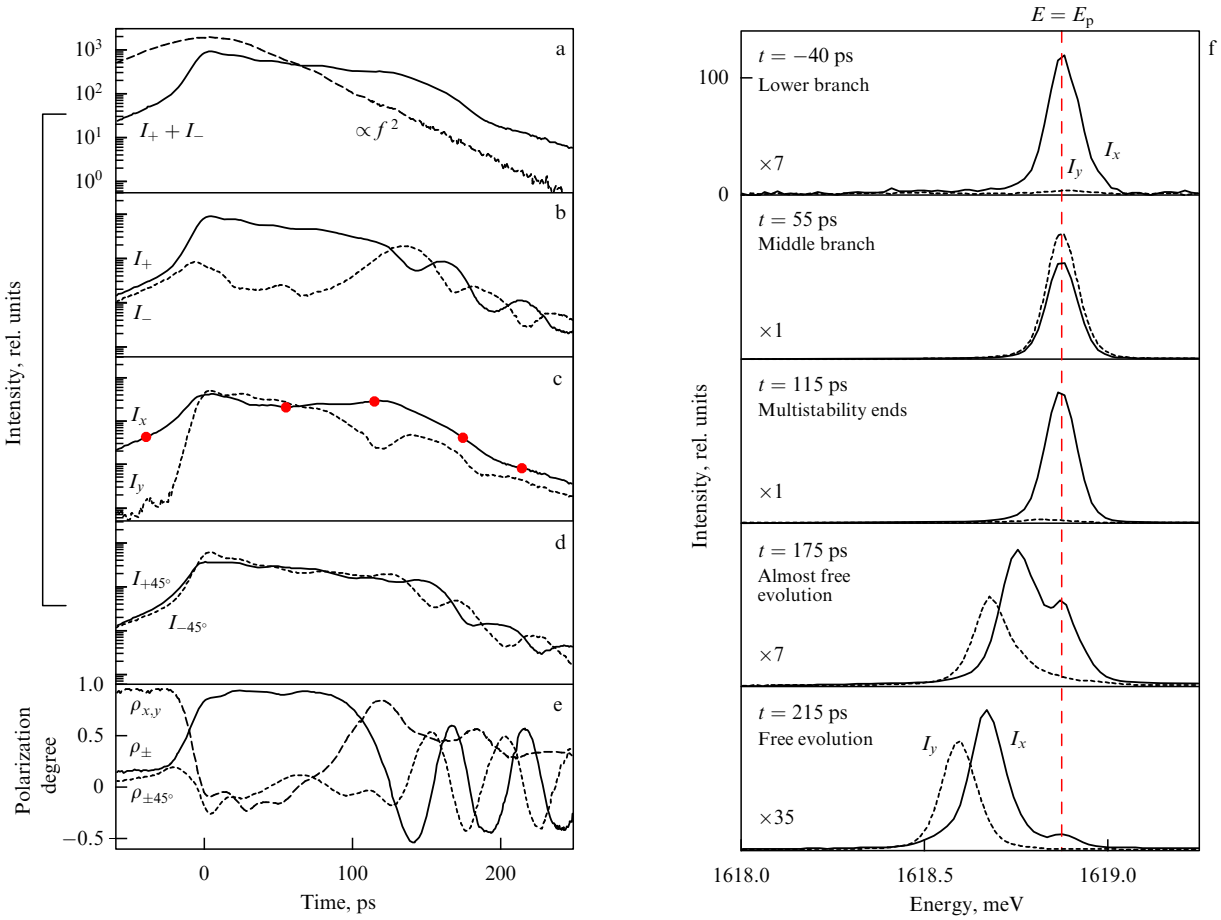

Figure 7. Dynamics of the polariton mode $k = 0$ under pulsed pumping (experiment [57]). (a) The pulse shape and the total transmission signal, (b–d) individual signal components in three Stokes bases, and (e) the corresponding degrees of polarization as functions of time. The pump is polarized linearly in the x direction. (f) Spectra of the components $I_{x,y} = |\psi_{x,y}|^2$ near the selected time instants marked by circles in Fig. c. The width of the spectra roughly corresponds to the hardware resolution (the actual width is less).

An irreversible violation of the spin balance is partly similar to the self-trapping of the Josephson transition [15, 133, 134, 137, 141, 142], but such an analogy would be too superficial. The absence of a reverse oscillation in our case does not come from nonlinearity, but rather from the fact that both components vary with the same forced frequency, while nonlinearity, on the contrary, provides a 'choice' of spin during the transition. It should be noted that as g/γ increases, a second possibility of symmetry breaking arises; namely, new stable solutions with diagonal linear polarizations emerge, due to which quantized vortices and dark solitons can form in the system [143].

7.2 Experiments

We now consider an experiment showing spin symmetry violation at $g \gtrsim \gamma$ [57] (Fig. 7). The sample, the characteristics of which were presented in Section 2, was grown using molecular beam epitaxy on a GaAs substrate opaque to light at a resonant frequency ($E_0 \approx 1.6$ eV). To perform a light transmission experiment, the substrate was removed in a rectangular region of 0.7×0.3 mm^2 by selective etching. This operation resulted in the emergence of a minor mechanical stress associated with the difference in the lattice periods of the layers that form the mirrors (the substrate stabilizes this system). As a result, a splitting of eigenmodes polarized along the [110] (x, upper level) and [1$\bar{1}$0] (y) axes arose; the etched area was originally oriented along the same axes.

The experiment was performed in an optical cryostat at a temperature of 2 K. The pump was provided by a mode-locked titanium-sapphire laser. The pulses had a duration of about 80 ps at half maximum intensity and a repetition rate of 8 MHz. A technique was used in which the conjugation of the laser and the detector (streak camera) made it possible to record a signal with a picosecond resolution, but the result is actually averaged over many individual pulses. A relatively wide beam was focused onto a spot 40 micrometers in size, and the signal shown in Fig. 7 was received from the center of the spot. The detuning D was 0.24 meV at $g \approx 0.08$ meV and $\gamma \approx 0.05$ meV; these parameters approximately correspond to Fig. 6c, d. The polarization was linear in the x direction; the 'seeding' degree of circular polarization that was required to reproduce the result in a series of pulses was 5%.

Figure 7a–e shows the evolution of the signal. Displayed are its intensity, the degree of circular polarization $\rho_\pm = \rho_c$, as well as $\rho_{x,y}$ and $\rho_{\pm 45^\circ}$, the degrees of linear polarization in the bases $\mathbf{e}_{x,y}$ and $\mathbf{e}_x \pm \mathbf{e}_y$ rotated one relative to the other by 45°,

$$\rho_{x,y} = \frac{|\psi_x|^2 - |\psi_y|^2}{|\psi_x|^2 + |\psi_y|^2}, \qquad \rho_{\pm 45^\circ} = \frac{\psi_x^* \psi_y + \psi_y^* \psi_x}{|\psi_x|^2 + |\psi_y|^2}. \tag{47}$$

The directly measured intensities $I = |\psi|^2$ of each of the polarization components ($I_\pm$, $I_{x,y}$, and $I_{\pm 45^\circ}$) are also plotted. Should the instantaneous values of all I be precisely

measured, the following relation would hold true:

$$\rho^2 \equiv \rho_{\pm}^2 + \rho_{x,y}^2 + \rho_{\pm 45^\circ}^2 = 1\,. \tag{48}$$

The value of ρ decreases if the contributions coming from individual pulses to the result are not the same. Signal depolarization is indicative of instability and sensitivity to small fluctuations.

Figure 7f shows spectra $I_{x,y}(E)$ near some selected time instants; $t = 0$ corresponds to the peak of the pulse. Spectra I_x and I_y were recorded separately. The hardware resolution was approximately 0.06 meV, due to which all the lines are greatly broadened. Of interest to us is only the location of the lines E_x and E_y, which, despite the broadening, is quite accurately determined using the weighted average spectra.

We consider the main stages in the evolution of the system during the pulse passage. The signal is initially polarized in the same way as the external field in the x direction, and a superlinear increase in its intensity can be observed, which is characteristic of the lower branch of solutions. Levels E_x and E_y are located at the pump frequency, as should always be the case if the amplitude f is a constant or changes relatively smoothly. It should be stressed that $E_{x,y}$ correspond to the frequencies of the condensate, and not the excitations shown in Fig. 6e.

Next, a signal jump occurs: its intensity increases by an order of magnitude in less than two 'lifetimes' $\tau = \hbar/\gamma$. At first, both spin components increase ($t \approx -20$ ps), but ψ_+ outraces and then strongly suppresses the ψ_- component which starts decreasing even at $t < 0$. As a result, the condensate proves to be locked in the state with right-handed circular polarization for about 100 ps. The same process may be, however, interpreted in an alternative way from the perspective of linear $I_{x,y}$ components. In this basis, the x component is enhanced earlier, since it corresponds to an eigenstate, whose polarization is the same as that of the external field and whose frequency is closer to the pump one at the pulse beginning. The state with polarization y could not be populated at all in the absence of nonlinearity. But, as in Fig. 6, it loses stability ($\mathrm{Im}\,\tilde{E}_y > 0$), while still having a noise-level amplitude, and as a result is exponentially amplified by two orders of magnitude over about the same time of 2τ.

The condensate proves to be sooner or later at the left boundary point of the middle branch. It will go down from there to the lower branch should the pulse be longer, but in our case it does not have enough time for this transition, since at each moment its amplitude is higher than that of the static solution $\bar{\psi}_{\pm}(f(t))$. The breaking of the middle branch is therefore similar to the interruption of pumping, and the system switches from forced evolution to a free one. The linear coupling between ψ_+ and ψ_- now manifests itself, first, in the splitting of the levels E_x and E_y that tend over time to eigenfrequencies $E_{\mathrm{LP}} \pm g/2$, and, second, in the oscillations of $\rho_{\pm}$ and $\rho_{\pm 45^\circ}$, an 'internal Josephson effect' [142]. The oscillation period T is routinely related to the coupling strength: $T = 2\pi\hbar/g$.

The fact that oscillations do not halt after more than 100 ps when the field density decreases by one and a half orders of magnitude is an indication of a long coherence time. However, now it would be incorrect to speak of the general condensate state of polaritons. The blue shift no longer compensates the inhomogeneities in the eigenenergy distribution, and, having lost connection with the external field, the condensate decomposes into islands whose further evolution is not the same [144]. The island that in our example provided the main contribution to the 'free' signal ($t > 115$ ps and $E_{x,y} < E_{\mathrm{p}}$) is a localized state with a relatively long lifetime, which is several times greater than τ for a plane wave. (Quasi-equilibrium condensates are known to also exhibit spatial fragmentation in the vicinity of the threshold [5, 7].)

Distinguishable oscillations at the trailing edge imply, in addition, that the system dynamics is almost the same in each individual pulse. The total polarization ρ is virtually equal to unity on the lower branch of solutions. It decreases to 0.75 at the transition point, where the system is unstable, but then returns to 0.95 on the middle branch to remain so until $t \approx 115$ ps. Due to condensate fragmentation, the system is sensitive to fluctuations, and after the moment $t \approx 115$ ps ρ linearly decreases over time to 0.5 at $t \approx 250$ ps.

The symmetry violation in the considered example was, in standard terms, an *explicit* one, i.e., originated from some finite seed that predetermined the transition. For a more stringent balance between the amplitudes $f_{\pm}$ in external pulses, the 'spin' outcome of each jump of the field becomes random.

Equations (1) well reproduce the behavior of the system up to the fragmentation stage, including all intensities, phases, and characteristic times. A detailed comparison of experiments and calculations is presented in [55, 56]. The transition to the uppermost (symmetric in spin) branch of stationary solutions was also explored in [55], while in [56] spatial effects in an inhomogeneous system were studied. If the problem is slightly complicated, new interesting phenomena may be found [129–131]. For example, the condensate can change the sign of circular polarization in a constant magnetic field $\mathbf{B} \parallel z$ depending on the pump amplitude, a phenomenon that was also experimentally confirmed in the pulsed regime [129]. In addition, it was predicted that transitions under the effect of fast acoustic perturbations are possible between the states whose symmetry is broken in opposite ways [130]. Finally, it is noteworthy that parity violation has recently been found in quasi-equilibrium polariton condensates, where it emerges as a result of interaction with an exciton reservoir [145, 146].

8. Chaos and a new order

8.1 Turbulence in optics

Evolution is predetermined in chaotic states by the initial conditions, but it is virtually unpredictable, since close trajectories quickly diverge. Nevertheless, an *attractor* in the phase space, to which they all tend, exists, being a complex object with a fractional dimension. Chaotic solutions have been found by E Lorenz in a model of atmospheric convection with only three degrees of freedom [147]. G Haken found an analogy between the Lorentz model and the Maxwell–Bloch system of equations for inverse-population media [148]. Many chaotic emitters have been created since then based, for example, on laser diodes [60]. It has been found recently that even the circular-polarization degree in their emission can vary randomly [149,150].

A more difficult task is to obtain spatiotemporal chaos, i.e., a state in which light resembles a turbulent fluid. It does not arise in coherent optics as easily as in hydrodynamics if strictly deterministic rather than stochastic processes are meant. In passing through the generation threshold in lasers, unstable modes compete with each other, and only a small

number of them eventually become *order parameters*; due to this, static dissipative patterns emerge in an extended system [86, 103]. A higher degree of complexity can be provided by external feedback when a chaotic signal emerging from the active medium returns there delayed in time [151]. Examples of such systems are ring resonators with a photo-amplifying element, in which turbulent radiation was first observed [152], or state-of-the art lasers with an external resonator [59, 153, 154]. However, feedback also results in additional correlations in the output signal those reduce its complexity [155]. Spatiotemporal chaos has also been found recently in a planar microcavity with a saturable absorber [156, 157]. Solitons and self-oscillations were evidenced in this system even earlier [158]; however, chaos was observed only in a one-dimensional strip on the sample.

All of these systems are 'laser' type devices that contain an active medium in which light is generated or amplified. There is also a simpler way to optical instability: self-focusing of a coherent field in a passive nonlinear medium that we have already mentioned as a possible cause of the blowup regimes. Dissipative structures [25] and chaos [159] are known to emerge in the system of equations (13) with $V<0$. However, while predicting an infinite self-focusing proceeding in a finite time in two- and three-dimensional systems at $f\to 0$ and $\gamma\to 0$ [107], such a model is no better than a crude illustration in the case of a gas of particles with a positive effective mass.

For a polariton system, when $V>0$ and the theory is accurate in the low-density limit, the emergence of chaos is hindered precisely because the particles repel each other. Random inhomogeneities in their distribution do not grow but tend to level during the particle's lifetime, while there is simply no amplification characteristic of 'lasers' ($\operatorname{Im} V$) or feedback loops. There is also no explicit way to generate new frequency harmonics, as in the Duffing equation with real-valued nonlinearity of the form $(\psi+\psi^*)^3$. If the system is internally homogeneous and is excited by a plane wave, it seemed for a long time that the only nontransient collective effect in it could only be pairwise break-up of the condensate. The model can be complicated to some extent by introducing strong inhomogeneity. For example, a transition to chaos was predicted in a Josephson junction with a tunnel coupling of two condensates with a certain nonlinear coupling of their spin components [160]. However, it is difficult or impossible to scale in space any inhomogeneity, such as a barrier between condensates (unless creating a discrete chain of condensates or something similar is meant), which complicates the transition to spatial turbulence.

8.2 Loop scattering mechanism

It has been found out recently that, despite the repulsion between particles and dissipation, system (1) allows spontaneous break-up of the homogeneous state and chaotic dynamics [53, 58]. This may occur if $g>4\gamma$, when higher-order interaction processes come into play. Previously we have considered the two-particle scattering with conserved spin and momentum, which can be symbolically represented by the diagram

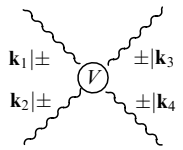

, where $\mathbf{k}_1+\mathbf{k}_2=\mathbf{k}_3+\mathbf{k}_4$, (49)

as well as the linear coupling of the spin components + and −:

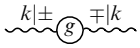

. (50)

The new scattering process, which is discussed below, has a loop form,

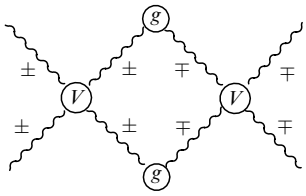

, (51)

in which the degeneracy of the unstable modes is lifted (Fig. 8) and spin inversion allowed.

Let us now determine the spectrum of above-condensate modes in the stationary state $\psi_\pm(t)=\bar\psi_\pm\exp(-\mathrm{i}E_\mathrm{p}t/\hbar)$. Repeating all the arguments given in Section 4 with consideration for two spin components, instead of the system of equations (17), we obtain

$$\begin{pmatrix} a_{11} & a_{12} & a_{13} & a_{14}\\ a_{21} & a_{22} & a_{23} & a_{24}\\ a_{31} & a_{32} & a_{33} & a_{34}\\ a_{41} & a_{42} & a_{43} & a_{44}\end{pmatrix}\begin{pmatrix}\tilde\psi_{+|+\mathbf{k}}\\ \tilde\psi^*_{+|-\mathbf{k}}\\ \tilde\psi_{-|+\mathbf{k}}\\ \tilde\psi^*_{-|-\mathbf{k}}\end{pmatrix}=\mathbf{0}\,, \tag{52}$$

where $a_{11}=2V|\bar\psi_+|^2+s-\lambda$, $a_{12}=V\bar\psi_+^2$, $a_{13}=g/2$, $a_{14}=0$, $a_{21}=-V\bar\psi_+^{*2}$, $a_{22}=-2V|\bar\psi_+|^2-s-\lambda$, $a_{23}=0$, $a_{24}=-g/2$, $a_{31}=g/2$, $a_{32}=0$, $a_{33}=2V|\bar\psi_-|^2+s-\lambda$, $a_{34}=V\bar\psi_-^2$, $a_{41}=0$, $a_{42}=-g/2$, $a_{43}=-V\bar\psi_-^{*2}$, $a_{44}=-2V|\bar\psi_-|^2-s-\lambda$,

$$s=E_\mathrm{LP}(\mathbf{k})-E_\mathrm{p}\,,\qquad \lambda=\tilde E-E_\mathrm{p}+\mathrm{i}\gamma\,, \tag{53}$$

$\tilde E=\tilde E(\mathbf{k})$ is the sought-for function. The equation $\det(\cdot)=0$ is biquadratic with respect to λ, yielding solutions of the form

$$\tilde E=E_\mathrm{p}-\mathrm{i}\gamma\pm\sqrt{\frac{P\pm\sqrt{Q}}{2}}\,. \tag{54}$$

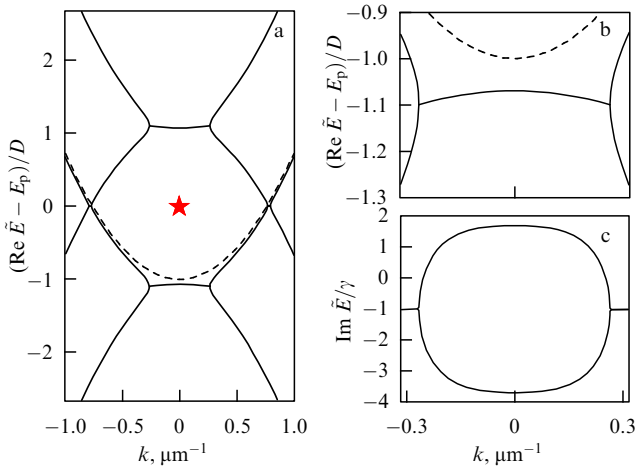

Figure 8. (a, b) Real and (c) imaginary parts of the Bogolyubov quasiparticle energy, $\operatorname{Re}\tilde E(k)$ and $\operatorname{Im}\tilde E(k)$, in a state with broken spin symmetry [58]. Figure b shows an enlarged part of Fig. a. The star in Fig. a indicates the condensate mode. Parameters: $\gamma=0.02$ meV, $g=10\gamma$, $D=E_\mathrm{p}-E_\mathrm{LP}(0)=15\gamma$, $\bar\psi_-=0$, and $V\bar\psi_+^2=D+g/2$ in accordance with Eqn (45); spectrum $E_\mathrm{LP}(k)$ is shown by the dashed curve.

In considering broken spin symmetry states, we assume that one of the $\bar{\psi}_\pm$ components vanishes completely, and for the remaining one we introduce the notation $\chi^2 = V|\bar{\psi}|^2$; then,

$$P = 2s^2 + 4s\chi^2 + 3\chi^4 + \frac{g^2}{2}\,, \tag{55}$$

$$Q = (4s\chi^2 + 3\chi^4)^2 + g^2(4s^2 + 8s\chi^2 + 3\chi^4)\,. \tag{56}$$

The homogeneous condensate state is unstable in the general case if $\operatorname{Im}\tilde{E} > 0$ for at least one k. There are two types of instability:

$$1)\quad Q > 0\,,\quad \text{but}\quad P \pm \sqrt{Q} < 0\,, \tag{57}$$

$$2)\quad Q < 0\,. \tag{58}$$

The first type is a direct pairwise break-up of the condensate. This instability is responsible for all the spontaneous effects discussed earlier, including those sensitive to spin [161, 162], and the parity violation itself (see Fig. 6). But if the parity is *already* violated, then the second type of instability may emerge in this last remaining homogeneous state, which is associated with higher-order scattering. It can be seen, for example, that only one term, $8sg^2\chi^2$, in Eqn (56) can be less than zero, and it is proportional to both V and g^2. Scattered modes can now be split in energy, but have at the same time a momentum equal to that of the condensate. Also, when populated, these modes restore the spin component that has disappeared owing to the symmetry breaking, even if this component is completely suppressed in the condensate. Having calculated the eigenstates, one can find, for example, that $\rho_c(k=0) \approx -0.6$ for the lower scattered mode shown in Fig. 8, although $\bar{\psi}_- = 0$ in the condensate.

Spectrum (54)–(56) displayed in Fig. 8 can be easily understood by superimposing the dispersion curves corresponding to states *6* and *1* in Fig. 2. The $\operatorname{Re}\tilde{E}(k)$ branches from the two components get close to each other in the combined picture near $k = 0$ and $E = E_p \pm D$, while for $g > 0$ they *join* in these places and form almost flat sections, as is shown in Fig. 8a. To this end, it is necessary in the general case that pair processes (49) with spins '+' and '−' match each other in energy near $k_{1,2,3,4} = 0$, while the connecting lines must have different signs of 'convexity' $\mathrm{d}^2E/\mathrm{d}k^2$. This is always the case when $\chi^2 = D + g/2$, i.e., in states with maximum spin asymmetry (see Eqn (45)) if the values of g and D are close to each other. Figure 9 explicitly shows the region of g and D in which asymmetric states are unstable. It is seen that instability of this type is only possible at $g/\gamma \gtrsim 4$.

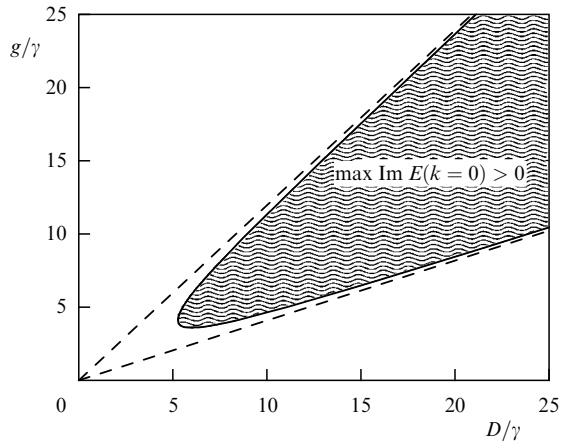

Figure 9. Parameters D and g (in units of γ) at which asymmetric states $\chi^2 = D + g/2$ are unstable [58].

8.3 Self-pulsations and deterministic chaos

Starting with an analysis of spontaneous parity violation (see Section 7), we have found another break-up process, this time occurring in an asymmetric state. As a result, there are no longer stable homogeneous solutions whatsoever in a finite interval f, and we arrive at a situation wherein the emergence of either inhomogeneous patterns or oscillations with new frequencies, $E \neq E_p$, which do not attenuate at $t \to \infty$, is inevitable. We consider the latter possibility using as an example the 'micropillar', where the system actually has only three degrees of freedom: $|\psi_+|$, $|\psi_-|$, and phase difference $\arg\psi_+^*\psi_-$ [53] (Fig. 10). The calculation was performed at $\gamma = 0.02$ meV, $g = 10\gamma$, and a relatively low detuning $D = 7.5\gamma$. For one pump intensity $f^2 = f_0^2$, the system behaves chaotically (Fig. 10a, b), while if $f^2 = 2.5f_0^2$, the oscillations become regular (Fig. 10c, d).

Chaos emerges due to a combination of nonlinear effects of two alternating types, (57) and (58). The 'internal' break-up $E_p \to E_p \pm D$ of the fields with high ρ_c restores the spin balance, which then breaks again in one direction or another. The system is sensitive to small deviations: its two trajectories, even those that are arbitrarily close near the equilibrium point (Π), quickly diverge, a behavior typical of chaotic states. The oscillations can shift in a more intense external field far from the point Π to become strictly periodic. However, such solutions can only be obtained if the detuning D is comparatively small, whereas at $D > g$, all solutions on most of the unstable interval f^2 exhibit chaos [53]. The average frequency of spin switching in those solutions is comparable with $\operatorname{Im}\tilde{E}/h$ and may be as high as 10^{11} Hz for GaAs-based structures.

8.4 Filaments

Chaos results in a loss of homogeneity in an extended system with continuous spectrum $E_{LP}(k)$, as a result of which new static solutions can form. The condensate breaks up in this case into many modes, and its momentum becomes indefinite in at least one direction. To estimate the scale of the inhomogeneity, we take into account that the frequencies of the scattered modes equal E_p in the case of the instability of the first type; therefore, their momenta are limited. Namely, direct break-up of the condensate is prohibited into modes $|\mathbf{k}| \geqslant k_{max}$, where

$$E_{LP}(k_{max}) - \frac{|g|}{2} = E_p\,. \tag{59}$$

The second type of instability does not shift the boundary k_{max}. If the characteristic width Δk of the k-space distribution of $|\psi|$ in is much smaller than k_{max}, the state of the condensate and the measure of its stability are virtually the same as in the single-mode (strictly homogeneous) case, i.e., the solution is unstable. Conversely, stabilization is only possible if the magnitudes of Δk and k_{max} are comparable. The lower limit of the spatial inhomogeneity scale a_{min} can be roughly estimated as $2/k_{max}$ [54]. The dispersion law has near $k = 0$ a parabolic form: $E_{LP}(k) \approx E_{LP}(0) + \hbar^2k^2/(2m_{LP})$; consequently,

$$a_{min} = \frac{2}{k_{max}} = \frac{2\hbar}{\sqrt{m_{LP}(g + 2D)}}\,. \tag{60}$$

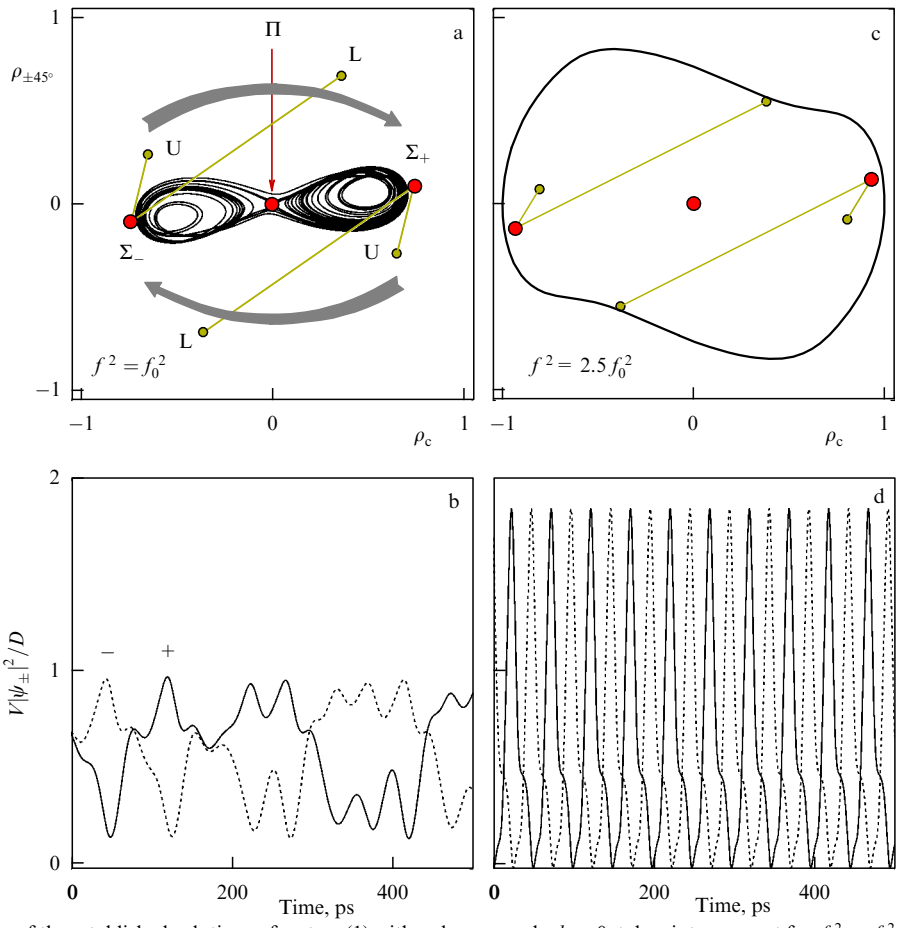

Figure 10. Fragments of the established solutions of system (1) with only one mode, $k = 0$, taken into account for $f^2 = f_0^2$ (a, b) and $f^2 = 2.5 f_0^2$ (c, d). Panels a and c show the trajectories in the coordinates ρ_c and $\rho_{\pm 45^\circ}$ (see formulas (11) and (47)) for 2000 ps; panels b, d display explicit functions $|\psi_\pm(t)|^2$. Points Π and $\Sigma_\pm$ correspond to symmetric and two asymmetric solutions of static equations (43); L and U are the lower and upper eigenstates of quasiparticles at points $\Sigma_\pm$: $\mathrm{Re}\,\tilde{E}_{L,U} \approx E_p \mp D$. Parameters: $\gamma = 0.02$ meV, $g = 10\gamma$, and $D = 7.5\gamma$.

The width a of the characteristic strips that form static solutions similar to those displayed in Fig. 11 usually lies in a range from $2a_{\min}$ to $4a_{\min}$. Calculations show that if the distribution of $|\psi|$ contains more homogeneous regions, it varies in time [53, 54].

It should be noted that filaments (thready structures) emerge in superconductors and condensates with quantized vortices [163], ordinary liquids with convection [164], and reaction-diffusion systems [165]. They may emerge in optics due to self-focusing of light in a passive [25, 159] or amplifying [166] nonlinear medium and in lasers with spatially variable pump [167, 168].

'Spin filaments' are in our case a compromise between tending to homogeneity (due to *defocusing*, i.e., repulsion of particles) and the fact that static homogeneous solutions are now forbidden in any two-dimensional region, the scale of which is significantly larger than $a_{\min}$. Being nonuniform in intensity, the solution cannot be uniform in spin; otherwise, we would return to the blowup regime described in Section 5. Calculations show, however, that the solution stabilizes when filaments with opposite polarizations alternate. Their thickness does not depend on the size of the entire system; however, as the size increases, differently oriented domains emerge in their distribution. This feature distinguishes the polariton system from reaction-diffusion models with spiral waves (the waves are 'straight' in our case), and, on the other hand, from liquids, in which the filament geometry, as a rule, crucially depends on the boundary conditions [165]. In a

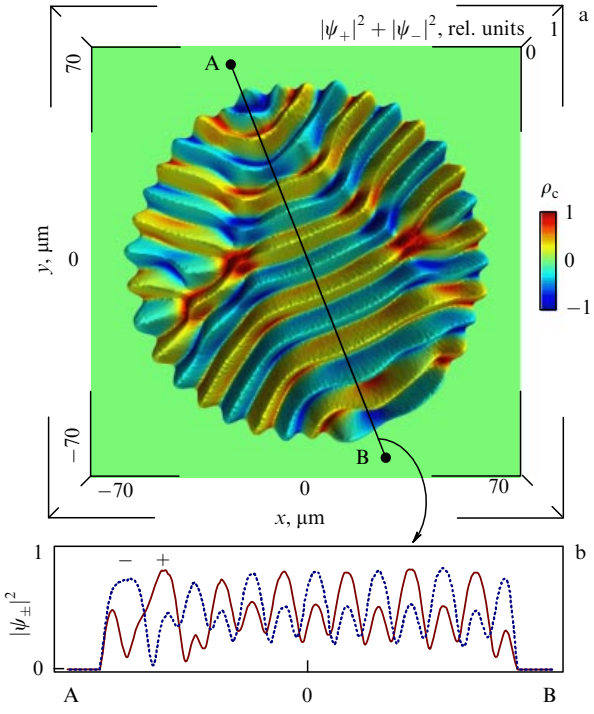

Figure 11. (Color online.) (a) Example of a steady-state static solution of system (1) [53]. Parameters γ, g, and D are the same as in Fig. 10. Zero boundary conditions are ensured by the steep increase in γ at $|\mathbf{r}| = 60$ μm. (b) Distribution of $|\psi_+|^2$ along a selected AB segment.

two-dimensional polariton system, long-range order is absent.

8.5 Dipolar spin network

The same instability which results in filaments in the case of a two-dimensional system gives rise in a one-dimensional system to a periodic pattern. Now, when polaritons do not even have a single free direction, a static solution can only be obtained if all inhomogeneities are the same and exactly balance each other. One-dimensionality in its literal sense is not required for this; a periodic chain also emerges in a flat system, which is excited, albeit, not over the entire area, but rather along a strip with a small transverse size $\sigma \lesssim a_{\min}$. Figure 12 shows an example of a solution with ring pumping: the initial SO(2) symmetry is broken, but a secondary-ordered and closed spin chain emerges in its stead. The polarizations in it alternate, and in between the nodes, where $\rho_c = 0$, the field intensity is significantly lower than at the points of maximum $|\rho_c|$.

The secondary, or internal, order in a quasi-one-dimensional system turns out to be a *rigid* one. In particular, it is now possible not only to describe such a system if the period and $|\psi_\pm|$ are known in some particular place, but to really control the entire chain, acting on any node, for example, using a second beam focused onto a spot whose diameter is less than $a_{\min}$. Figure 12b shows the result of such a numerical experiment. The intense second beam, the effect of which does not extend beyond one node, inverts ρ_c in it, after which the spins in all nodes also flip one by one. Such a process resembling signal transmission slows down as the ratio $\sigma/a_{\min}$ increases and vanishes when the system loses its periodicity.

The long-range order is completely uncharacteristic of systems with repulsion of particles whose lifetime is finite. Ordering in an external field is trivial, and nonlinearity does not change the situation, even if some kind of fluctuation triggers a transition between different branches of solutions, precisely because it is nothing but a transitional process, whereas the solutions themselves are homogeneous. However, strong long-range order emerges in a somewhat paradoxical way along with chaos. The system is ordered because it is 'strained' by the instabilities that compensate each other at the boundaries of nodes with opposite spins.

Thus, the condensate no longer resembles a gas, but a solid — a dipolar crystal. Similar patterns could emerge in a periodic external field that forms a coupled lattice of atomic condensates. The term *supersolid* is increasingly widely used in exploring such systems. It was understood earlier as a *superfluid solid*, referring to the propagation of vacancies that emerge in a real crystal due to zero-point oscillations and propagate without dissipation [169]. No convincing evidence for this has been obtained yet, but a similar transport of excitations in externally induced lattices is now under active study [170, 171].

In a polariton system, where the lattice itself spontaneously forms from a homogeneous medium, transport processes also occur that are not reduced to a response to an external disturbance. For example, as g/γ increases, the dipolar chain becomes *bistable*, since the spin symmetry can be broken in two ways. Namely, neighboring nodes throughout the chain can have either circular, $\rho_c \sim \pm 1$, or mixed-linear, $\rho_{\pm 45^\circ} \sim \pm 1$, polarizations. Solitons with second-type polarization can propagate along the first-type chain and vice versa (see Supplemental Material to [54]). The soliton is

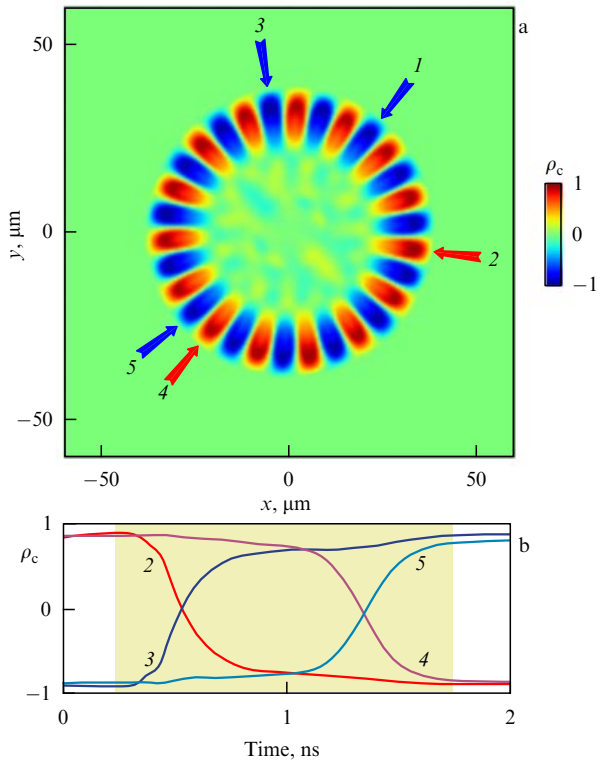

Figure 12. (Color online.) (a) Steady-state solution with a ring distribution of the external field amplitude $f_+(\mathbf{r}) = f_-(\mathbf{r}) \propto \exp[(|\mathbf{r}| - R_0)^2/(2\sigma^2)]$, where $R_0 = 30$ μm, $\sigma = 5$ μm [54]. (b) Inversion of spins due to the effect of the second beam with right-handed circular polarization focused onto a spot 1 μm in diameter at point *1*. The evolution of ρ_c is shown at checkpoints *2–5*; the time interval during which the second beam is applied is shaded. Parameters γ, g, and D are the same as for Figs 10 and 11.

similar to a crystal defect. It springs up spontaneously in a particular node and moves without attenuation in one direction or another at a constant speed of about 0.3 μm ps^{-1}, while its polarization is determined at each time moment by the current node of the main lattice according to the rule $\mathrm{sgn}\rho_c = \mathrm{sgn}\,\rho_{\pm 45^\circ}$. Similar effects exist in a two-dimensional system. As a rule, one of two base pairs, $I_\pm$ or $I_{\pm 45^\circ}$, alternates in space and thereby forms a lattice, while the other pair is only visible in the places where filaments branch or bend, as seen in Fig. 11. Such dislocations can move like solitons, resulting in spatiotemporal chaos [53].

8.6 Chimera states

We have found that, if a solution is stable, the polariton momentum is not defined in at least one direction: $\Delta k \sim k_{\max}$. Spin dipoles are similar in this sense to the simplest electric dipole, a hydrogen atom that exists due to the uncertainty of electron momentum. However, stable states are not always formed, but only if the energy is relatively low. To obtain a stable periodic chain in a system with some g, quantities $D(g)$ and then $f(g, D)$ should be chosen close to the lower boundary of the $Q < 0$ region, where loop scattering is in effect (see Section 8.2). By contrast, with increasing energy one can pass from a stable state to space-time turbulence, and this can be done in different ways.

The easiest way is to increase f. Then, polaritons increasingly more strongly repel each other, and their distribution tends to become more homogeneous and, as a result, loses stability. Solitons arise in the spin network.

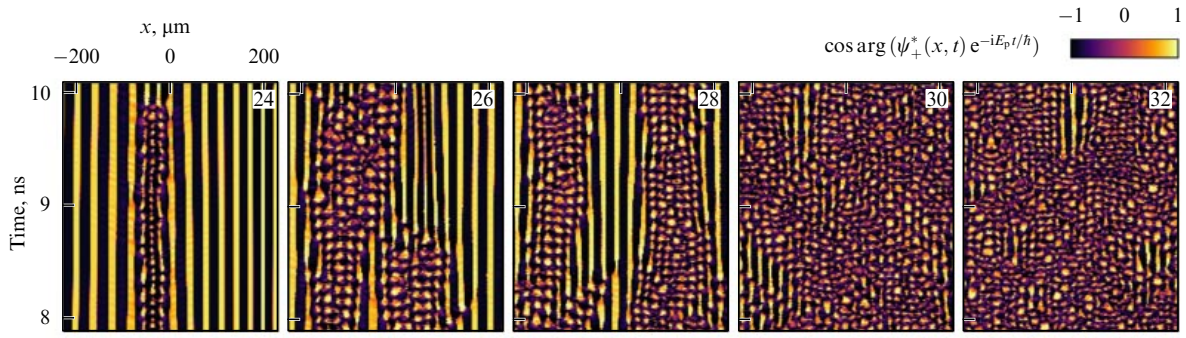

Figure 13. (Color online.) Series of solutions of one-dimensional equations (1) with periodic boundary conditions obtained with a simultaneous increase in mutually equal g and D [54]. The numbers on each plot indicate the ratio g/γ at $\gamma = 5$ μeV. The external-field intensity f^2 always matches the center of the unstable interval. The color scale corresponds to the cosine of the phase difference between ψ_+ and the external field. Evolution is shown after 8 ns to exclude transient effects related to establishing the solutions with time.

Multiplying and colliding, they make all nodes jitter. The nodes themselves are united into clusters in which one amplitude, $|\psi_+|$ or $|\psi_-|$, is on average larger than the other. The unstable interval f is limited on both sides, and the system smoothly tends at its end to one of the homogeneous solutions; if f increases further, spin symmetry is restored. Thus, as f increases, the system loses its long-range order due to the blurring of the boundaries between neighboring nodes, a phenomenon that is similar to the heating and melting of a crystal.

On the other hand, energy can be increased by increasing the detuning $D = E_\mathrm{p} - E_\mathrm{LP}$. In this case, in order not to go beyond the boundaries of the region that is of interest to us, i.e., $Q < 0$, it is necessary to concurrently increase g (see Fig. 9) and f (see (43) and (45)). As g increases, the spin components suppress each other more strongly; therefore, the discrete structure of the network is retained for a long time, even despite an increase in $|\psi|$. Figure 13 shows a series of solutions in which mutually equal D and g are gradually increased.

All chain nodes are now divided into two groups. In one, they are stable and fully synchronized. The frequency of field oscillations at any node is equal to $E_\mathrm{p}/\hbar$, and if the polarizations coincide in two of them, then the phases coincide as well. The nodes of which the other group consists oscillate chaotically. It is noteworthy that the two subsystems coexist, without being mixed or suppressing each other. The length of unicolor vertical stripes, i.e., coherence time, displayed in the first three images in Fig. 13 almost everywhere turns out to be either extremely small ($\sim\hbar/g$) or indefinitely large. At the beginning of a series, dephased nodes look like random defects in a periodic lattice, whereas at the end only small fragments of the lattice itself arise for a short time from a turbulent medium, but even then they are synchronized with good accuracy.

The effect of *intermittency*, or alternation of order and disorder on the way to turbulence, is well known [172]. However, order and disorder, while alternating in our case in separate nodes, are balanced across the entire system. Calculations show that the size ratio of the two subsystems stabilizes as the network length increases, i.e., a solution with a certain amount of disorder is structurally stable. Very similar solutions have been found in [61] in the model of phase oscillators with nonlocal interaction (2). The term *chimera states* was soon coined for such systems [62], because their subsystems seem incompatible, like a liquid and a crystal at an ultra-low temperature. (More understandable in comparison with Fig. 13 would be a gradual growth of fluctuations in all nodes, and, in the case of a transition to chaos, intermittency in the general state of the entire system.)

Similar structures emerge in the emission of lasers with optoelectronic feedback [66, 67]. This system features, in contrast, a time 'nonlocality': unlike (2), its evolution equation includes a time integral, but the solutions also have two subsystems, are structurally stable, and allow a transition from global order to turbulence. The calculated results have been experimentally confirmed, and, in addition, chimera states have been found in various other systems with nonlocal coupling (see, e.g., [68–70] and reviews [64, 65]). On the one hand, all interactions in Eqns (1) for the polariton system are local and 'instantaneous', but, on the other hand, the solutions sometimes exhibit a strong long-range order, as is displayed in Fig. 12. It is not clear at the moment whether such an effectively nonlocal coupling can be explicitly described by analogy to model (2).

9. Conclusions

Polariton systems are of interest in view of macroscopically coherent states that emerge in two ways: in a quasi-equilibrium way or in a resonant field. Since the polariton lifetime is not large, optical pumping is also required in the first case; however, it does not directly excite polaritons, but creates an exciton reservoir from which particles scatter to the ground state. Such a condensate is formed with violation of gauge symmetry, and quantized vortices [16–19], the excitations that were predicted long ago and first found in superconductors and atomic gases, spontaneously emerge in the condensate. It may be asserted that the condensate is in this case internally ordered.

In the case of a condensate excited by a resonant light wave, the phase and all properties are, on the contrary, usually imposed by the external field, so that the condensate behaves like a forced oscillator everywhere with the exception of a few critical points. It was long thought that such a condensate per se is a very simple system, which, however, can be easily complicated by setting in an arbitrary way the pump $f_\pm(\mathbf{r}, t)$ or potential $E_\mathrm{LP}(\mathbf{r}, -\mathrm{i}\hbar\nabla, t)$. The latter can be controlled in real samples by acoustic waves or magnetic field or by creating tunnel-coupled traps, lattices, etc. Many spectacular nonlinear effects come into being this way, although they are usually different from the behavior of

atomic or exciton Bose–Einstein condensates with free phases.

A number of recent studies have shown, however, that sometimes even a perfectly homogeneous polariton system excited by a plane wave features a relatively free evolution instead of forced oscillations. In the regime with blowup, a multitude of wave modes start showing a strongly correlated behavior. If the internal (spin) degree of freedom is taken into account, it may turn out that homogeneous states are, in principle, forbidden in a finite interval of f; the momentum then becomes undefined, and all features of the system alter dramatically. It exhibits long-range order and turbulence, self-oscillations, lattices, filaments, and chimera states; solitons and vortices can also be spontaneously generated [143]. The *secondary-ordered* polariton system actually resembles a condensate rather than a set of forced oscillators, since its order and disorder are balanced, however, the origin of the disorder is purely dynamical rather than thermal.

Acknowledgments

The author is grateful to V D Kulakovskii, N A Gippius, and S G Tikhodeev for numerous discussions of the entire set of problems reviewed here. The study of the manifestations of the regime with blowup in an effectively spinless exciton-polariton system was supported by grants 16-02-01172 and 19-02-00988 from the Russian Foundation for Basic Research. Recent work related to self-oscillations resulting from spontaneous spin-symmetry breaking was supported by the Russian Science Foundation (grant no. 19-72-30003).

References

1. Hopfield J J *Phys. Rev.* **112** 1555 (1958)
2. Weisbuch C et al. *Phys. Rev. Lett.* **69** 3314 (1992)
3. Yamamoto Y, Tassone T, Cao H *Semiconductor Cavity Quantum Electrodynamics* (Berlin: Springer, 2000)
4. Kavokin A V et al. *Microcavities* 2nd ed. (Oxford: Oxford Univ. Press, 2017)
5. Deng H, Haug H, Yamamoto Y *Rev. Mod. Phys.* **82** 1489 (2010)
6. Pitaevskii L, Stringari S *Bose–Einstein Condensation and Superfluidity* (Oxford: Oxford Univ. Press, 2016)
7. Kasprzak J et al. *Nature* **443** 409 (2006)
8. Balili R et al. *Science* **316** 1007 (2007)
9. Baumberg J J et al. *Phys. Rev. Lett.* **101** 136409 (2008)
10. Plumhof J D et al. *Nature Mater.* **13** 247 (2014)
11. Daskalakis K S et al. *Nature Mater.* **13** 271 (2014)
12. Timoffeev V B *Semiconductors* **46** 843 (2012); *Fiz. Tekh. Poluprovodn.* **46** 865 (2012)
13. Carusotto I, Ciuti C *Rev. Mod. Phys.* **85** 299 (2013)
14. Lagoudakis K G et al. *Phys. Rev. Lett.* **105** 120403 (2010)
15. Abbarchi M et al. *Nature Phys.* **9** 275 (2013)
16. Lagoudakis K G et al. *Nature Phys.* **4** 706 (2008)
17. Keeling J, Berloff N G *Phys. Rev. Lett.* **100** 250401 (2008)
18. Amo A et al. *Science* **332** 1167 (2011)
19. Tosi G et al. *Nature Commun.* **3** 1243 (2012)
20. Berloff N G et al. *Nature Mater.* **16** 1120 (2017)
21. Keldysh L V "Kogerentnoe sostoyanie eksitonov" ("Coherent state of excitons"), in *Problemy Teoreticheskoi Fiziki. Pamyati Igorya Evgen'evicha Tamma* (Problems of Theoretical Physics. In Memory of Igor Evgenievich Tamm) (Ed. V I Ritus) (Moscow: Nauka, 1972) p. 433
22. Keldysh L V *Phys. Usp.* **60** 1180 (2017); *Usp. Fiz. Nauk* **187** 1273 (2017)
23. Elesin V F, Kopaev Yu V *Sov. Phys. JETP* **36** 767 (1973); *Zh. Eksp. Teor. Fiz.* **63** 1447 (1972)
24. Baas A et al. *Phys. Rev. Lett.* **96** 176401 (2006)
25. Lugiato L A, Lefever R *Phys. Rev. Lett.* **58** 2209 (1987)
26. Gippius N A et al. *Europhys. Lett.* **67** 997 (2004)
27. Baas A et al. *Phys. Rev. A* **69** 023809 (2004)
28. Gippius N A et al. *Phys. Rev. Lett.* **98** 236401 (2007)
29. Shelykh I A, Liew T C H, Kavokin A V *Phys. Rev. Lett.* **100** 116401 (2008)
30. Gavrilov S S et al. *JETP* **110** 825 (2010); *Zh. Eksp. Teor. Fiz.* **137** 943 (2010)
31. Paraïso T K et al. *Nature Mater.* **9** 655 (2010)
32. Sarkar D et al. *Phys. Rev. Lett.* **105** 216402 (2010)
33. Adrados C et al. *Phys. Rev. Lett.* **105** 216403 (2010)
34. Amo A et al. *Nature Photon.* **4** 361 (2010)
35. Cerna R et al. *Nature Commun.* **4** 2008 (2013)
36. Stevenson R M et al. *Phys. Rev. Lett.* **85** 3680 (2000)
37. Butté R et al. *Phys. Rev. B* **68** 115325 (2003)
38. Ciuti C, Schwendimann P, Quattropani A *Semicond. Sci. Technol.* **18** S279 (2003)
39. Gippius N A, Tikhodeev S G *J. Phys. Condens. Matter* **16** S3653 (2004)
40. Whittaker D M *Phys. Rev. B* **71** 115301 (2005)
41. Krizhanovskii D N et al. *Phys. Rev. Lett.* **97** 097402 (2006)
42. Demenev A A et al. *Phys. Rev. Lett.* **101** 136401 (2008)
43. Krizhanovskii D N et al. *Phys. Rev. B* **77** 115336 (2008)
44. Ballarini D et al. *Phys. Rev. Lett.* **102** 056402 (2009)
45. Ballarini D et al. *Nature Commun.* **4** 1778 (2013)
46. Bogolubov N *J. Phys. USSR* **11** 23 (1947); Bogolyubov N N *Izv. Akad. Nauk SSSR Ser. Fiz.* **11** 77 (1947); https://ufn.ru/dates/pdf/j_phys_ussr/j_phys_ussr_1947_11_1/3_bogolubov_j_phys_ussr_1947_11_1_23.pdf
47. Carusotto I, Ciuti C *Phys. Rev. Lett.* **93** 166401 (2004)
48. Amo A et al. *Nature Phys.* **5** 805 (2009)
49. Lerario G et al. *Nature Phys.* **13** 837 (2017)
50. Gavrilov S S *Phys. Rev. B* **90** 205303 (2014)
51. Gavrilov S S et al. *Phys. Rev. B* **92** 205312 (2015)
52. Whittaker C E et al. *Phys. Rev. X* **7** 031033 (2017)
53. Gavrilov S S *Phys. Rev. B* **94** 195310 (2016)
54. Gavrilov S S *Phys. Rev. Lett.* **120** 033901 (2018)
55. Gavrilov S S et al. *Appl. Phys. Lett.* **102** 011104 (2013)
56. Sekretenko A V et al. *Phys. Rev. B* **88** 205302 (2013)
57. Gavrilov S S et al. *Phys. Rev. B* **90** 235309 (2014)
58. Gavrilov S S *JETP Lett.* **105** 200 (2017); *Pis'ma Zh. Eksp. Teor. Fiz.* **105** 187 (2017)
59. Argyris A et al. *Nature* **438** 343 (2005)
60. Sciamanna M, Shore K A *Nature Photon.* **9** 151 (2015)
61. Kuramoto Y, Battogtokh D *Nonlin. Phenom. Complex Syst.* **5** 380 (2002)
62. Abrams D M, Strogatz S H *Phys. Rev. Lett.* **93** 174102 (2004)
63. Hagerstorm A M et al. *Nature Phys.* **8** 658 (2012)
64. Panaggio M J, Abrams D M *Nonlinearity* **28** R67 (2015)
65. Omel'chenko O E *Nonlinearity* **31** R121 (2018)
66. Larger L, Penkovsky B, Maistrenko Yu *Nature Commun.* **6** 7752 (2015)
67. Larger L, Penkovsky B, Maistrenko Yu *Phys. Rev. Lett.* **111** 054103 (2013)
68. Martens E A et al. *Proc. Natl. Acad. Sci. USA* **110** 10563 (2013)
69. Tinsley M R, Nkomo S, Showalter K *Nature Phys.* **8** 662 (2012)
70. Majhi S et al. *Phys. Life Rev.* **28** 100 (2019)
71. Andrzejak R G et al. *Sci. Rep.* **6** 23000 (2016)
72. Keldysh L V, Kozlov A N *Sov. Phys. JETP* **27** 521 (1968); *Zh. Eksp. Teor. Fiz.* **54** 978 (1968)
73. Snoke D, Kavoulakis G M *Rep. Prog. Phys.* **77** 116501 (2014)
74. Savona V et al. *Phys. Rev. B* **49** 8774 (1994)
75. Messin G et al. *Phys. Rev. Lett.* **87** 127403 (2001)
76. Sun Y et al. *Nature Phys.* **13** 870 (2017)
77. Sibeldin N N *Phys. Usp.* **60** 1147 (2017); *Usp. Fiz. Nauk* **187** 1236 (2017)
78. Ciuti C et al. *Phys. Rev. B* **58** 7926 (1998)
79. Vladimirova M et al. *Phys. Rev. B* **82** 075301 (2010)
80. Sekretenko A V, Gavrilov S S, Kulakovskii V D *Phys. Rev. B* **88** 195302 (2013)
81. Shelykh L A et al. *Semicond. Sci. Technol.* **25** 013001 (2010)
82. Voronova N S, Elistratov A A, Lozovik Yu E *Phys. Rev. Lett.* **115** 186402 (2015)
83. Gippius N A et al. *Phys. Usp.* **48** 306 (2005); *Usp. Fiz. Nauk* **175** 327 (2005)

84. Gavrilov S S, Tikhodeev S G *JETP Lett*. **94** 647 (2011); *Pis'ma Zh. Eksp. Teor. Fiz*. **94** 690 (2011)
85. Gibbs H M, McCall S L, Venkatesan T N C *Phys. Rev. Lett*. **36** 1135 (1976)
86. Haken H *Synergetics. An Introduction. Nonequilibrium Phase Transitions and Self-Organization in Physics, Chemistry, and Biology* (Springer Series in Synergetics, Vol. 1) (Berlin: Springer, 1983)
87. Demenev A A, Gavrilov S S, Kulakovskii V D *Phys. Rev. B* **81** 035328 (2010)
88. Gavrilov S S et al. *JETP Lett*. **92** 171 (2010); *Pis'ma Zh. Eksp. Teor. Fiz*. **92** 194 (2010)
89. Vishnevsky D V et al. *Phys. Rev. B* **85** 155328 (2012)
90. Gavrilov S S et al. *Phys. Rev. B* **85** 075319 (2012)
91. Wouters M et al. *Phys. Rev. B* **87** 045303 (2013)
92. Uvarov A V et al. *Phys. Rev. A* **99** 033837 (2019)
93. Gavrilov S S, Gippius N A *Phys. Rev. B* **86** 085317 (2012)
94. Akimov A V et al. *Phys. Rev. Lett*. **97** 037401 (2006)
95. Scherbakov A V et al. *Phys. Rev. B* **78** 241302(R) (2008)
96. Krizhanovskii D N et al. *Phys. Rev. B* **87** 155423 (2013)
97. Liew T C H, Kavokin A V, Shelykh I A *Phys. Rev. Lett*. **101** 016402 (2008)
98. Egorov O A et al. *Phys. Rev. Lett*. **102** 153904 (2009)
99. Egorov O A, Skryabin D V, Lederer F *Phys. Rev. B* **84** 165305 (2011)
100. Sich M et al. *Nature Photon*. **6** 50 (2012)
101. Sich M et al. *Phys. Rev. Lett*. **112** 046403 (2014)
102. Gavrilov S S *J. Phys. Conf. Ser*. **1164** 012014 (2019)
103. Haken H *Rev. Mod. Phys*. **47** 67 (1975)
104. Gavrilov S S et al. *JETP Lett*. **101** 7 (2015); *Pis'ma Zh. Eksp. Teor. Fiz*. **101** 9 (2015)
105. Brichkin A S et al. *Phys. Rev. B* **92** 125155 (2015)
106. McLaughlin D W et al. *Phys. Rev. A* **34** 1200 (1986)
107. Landman M J et al. *Phys. Rev. A* **38** 3837 (1988)
108. Flayac H, Savona V *Phys. Rev. A* **95** 043838 (2017)
109. Liew T C H, Rubo Y G *Phys. Rev. B* **97** 041302(R) (2018)
110. Wang T et al. *Phys. Rev. A* **92** 012316 (2015)
111. Karr J Ph et al. *Phys. Rev. A* **69** 031802(R) (2004)
112. Savvidis P G et al. *Phys. Rev. Lett*. **84** 1547 (2000)
113. Ciuti C et al. *Phys. Rev. B* **62** R4825 (2000)
114. Baumberg J J et al. *Phys. Rev. B* **62** R16247 (2000)
115. Kulakovskii V D et al. *Nanotechnology* **12** 475 (2001)
116. Whittaker D M *Phys. Rev. B* **63** 193305 (2001)
117. Ciuti C, Schwendimann P, Quattropani A *Phys. Rev. B* **63** 041303(R) (2001)
118. Gavrilov S S et al. *JETP* **104** 715 (2007); *Zh. Eksp. Teor. Fiz*. **131** 819 (2007)
119. Demenev A A et al. *Phys. Rev. B* **79** 165308 (2009)
120. Kulakovskii V D et al., in *Exciton Polaritons in Microcavities* (Springer Series in Solid-State Sciences, Vol. 172, Eds D Sanvitto, V Timofeev) (Berlin: Springer, 2012) p. 43
121. Maslova N S, Johne R, Gippius N A *JETP Lett*. **86** 126 (2007); *Pis'ma Zh. Eksp. Teor. Fiz*. **86** 135 (2007)
122. Johne R, Maslova N S, Gippius N A *Solid State Commun*. **149** 496 (2009)
123. Maslova N S, Johne R, Gippius N A *JETP Lett*. **89** 614 (2009); *Pis'ma Zh. Eksp. Teor. Fiz*. **89** 718 (2009)
124. Bozat Ö, Savenko I G, Shelykh I A *Phys. Rev. B* **86** 035413 (2012)
125. Rodriguez S R K et al. *Phys. Rev. Lett*. **118** 247402 (2017)
126. Demenev A A, Gavrilov S S, Kulakovskii V D *Phys. Rev. B* **84** 085305 (2011)
127. Demenev A A, Gavrilov S S, Kulakovskii V D *JETP Lett*. **95** 38 (2012); *Pis'ma Zh. Eksp. Teor. Fiz*. **95** 42 (2012)
128. Carusotto I et al. *Phys. Rev. Lett*. **97** 260403 (2006)
129. Gavrilov S S et al. *Phys. Rev. B* **87** 201303(R) (2013)
130. Gavrilov S S, Demenev A A, Kulakovskii V D *JETP Lett*. **100** 817 (2015); *Pis'ma Zh. Eksp. Teor. Fiz*. **100** 923 (2015)
131. Gavrilov S S, Kulakovskii V D *JETP Lett*. **104** 827 (2016); *Pis'ma Zh. Eksp. Teor. Fiz*. **104** 849 (2016)
132. Josephson B *Phys. Lett*. **1** 251 (1962)
133. Raghavan S et al. *Phys. Rev. A* **59** 620 (1999)
134. Albiez M et al. *Phys. Rev. Lett*. **95** 010402 (2005)
135. Cataliotti F S et al. *Science* **293** 843 (2001)
136. Levy S et al. *Nature* **449** 579 (2007)
137. Magnusson E B et al. *Phys. Rev. B* **82** 195312 (2010)
138. Read D, Rubo Yu G, Kavokin A V *Phys. Rev. B* **81** 235315 (2010)
139. Zhang C, Jin G *Phys. Rev. B* **84** 115324 (2011)
140. Pavlovic G, Malpuech G, Shelykh I A *Phys. Rev. B* **87** 125307 (2013)
141. Sarchi D et al. *Phys. Rev. B* **77** 125324 (2008)
142. Shelykh I A et al. *Phys. Rev. B* **78** 041302(R) (2008)
143. Gavrilov S S, arXiv:1909.10050
144. Demenev A A et al. *Phys. Rev. B* **94** 195302 (2016)
145. Ohadi H et al. *Phys. Rev. X* **5** 031002 (2015)
146. Askitopoulos A et al. *Phys. Rev. B* **93** 205307 (2016)
147. Lorenz E N *J. Atmos. Sci*. **20** 130 (1963)
148. Haken H *Phys. Lett. A* **53** 77 (1975)
149. Virte M et al. *Nature Photon*. **7** 60 (2013)
150. Virte M, Panajotov K, Sciamanna M *Phys. Rev. A* **87** 013834 (2013)
151. Ikeda K, Daido H, Akimoto O *Phys. Rev. Lett*. **45** 709 (1980)
152. Arecchi F T et al. *Phys. Rev. Lett*. **65** 2531 (1990)
153. Vicente R et al. *IEEE J. Quantum Electron*. **41** 541 (2005)
154. Albert F et al. *Nature Commun*. **2** 366 (2011)
155. Rontani D et al. *Opt. Lett*. **32** 2960 (2007)
156. Selmi F et al. *Phys. Rev. Lett*. **116** 013901 (2016)
157. Coulibaly S et al. *Phys. Rev. A* **95** 023816 (2017)
158. Elsass T et al. *Eur. Phys. J. D* **59** 91 (2010)
159. Ferré M A et al. *Eur. Phys. J. D* **71** 172 (2017)
160. Solnyshkov D D et al. *Phys. Rev. B* **80** 235303 (2009)
161. Krizhanovskii D N et al. *Phys. Rev. B* **73** 073303 (2006)
162. Solnyshkov D D et al. *Phys. Rev. B* **77** 045314 (2008)
163. Aranson I S, Kramer L *Rev. Mod. Phys*. **74** 99 (2002)
164. Bohr T et al. *Dynamical Systems Approach to Turbulence* (Cambridge: Cambridge Univ. Press, 1998)
165. Cross M C, Hohenberg P C *Rev. Mod. Phys*. **65** 851 (1993)
166. Couairon A, Mysyrowicz A *Phys. Rep*. **441** 47 (2007)
167. de Valcárcel G J, Staliunas K *Phys. Rev. E* **67** 026604 (2003)
168. de Valcárcel G J, Staliunas K *Phys. Rev. Lett*. **105** 054101 (2010)
169. Boninsegni M, Prokof'ev N V *Rev. Mod. Phys*. **84** 759 (2012)
170. Léonard J et al. *Nature* **543** 87 (2017)
171. Li J-R et al. *Nature* **543** 91 (2017)
172. Pomeau Y, Manneville P *Commun. Math. Phys*. **74** 189 (1980)